Diversity and Distributions

WILEY

Diversity and Distributions

RESEARCH ARTICLE OPEN ACCESS

Population Genetic Structure and Colonisation History of the Widely Distributed Mangrove *Avicennia marina* Across the Western Indian Ocean

Ludwig Triest[1] | Tim Sierens[2] | Nico Koedam[1,3,4,5] | Dennis De Ryck[1,2] | Farid Dahdouh-Guebas[1,3] | Tom Van der Stocken[2]

[1]Systems Ecology and Resource Management Research Unit (SERM), Department of Organism Biology, Université Libre de Bruxelles—ULB, Brussels, Belgium | [2]Ecology, Evolution and Genetics (bDIV) Research Group, Biology Department, Vrije Universiteit Brussel (VUB), Brussels, Belgium | [3]Mangrove Specialist Group (MSG), Species Survival Commission (SSC), International Union for the Conservation of Nature (IUCN), Gland, Switzerland | [4]Marine Biology Research Group, Universiteit Gent, Gent, Belgium | [5]Centre for Environmental Sciences (CMK), Universiteit Hasselt, Diepenbeek, Belgium

Correspondence: Ludwig Triest (ltriest@vub.be)

Received: 18 July 2025 | **Revised:** 11 October 2025 | **Accepted:** 11 January 2026

Keywords: conservation | dispersal | genetic differentiation | genetic diversity | microsatellites | migration | ocean currents | phylogeography | Pleistocene

ABSTRACT

Aim: *Avicennia marina* is a widely distributed mangrove species and a major constituent of Indo-West Pacific mangroves. To understand spatial patterns of genetic diversity in this species, and the role of ocean currents and historical events in shaping these patterns, we examined population genetic structure, maternal phylogeography, and colonisation history across the species' Western Indian Ocean range.

Location: Western Indian Ocean, including 34 populations of Kenya, Tanzania, Mozambique, South Africa, Madagascar, Mayotte Island, Europa Island, Aldabra Atoll and Granitic Seychelles; outgroups of the Red Sea and southeast Asia.

Taxon: *Avicennia marina* (Forssk.) Vierh.

Methods: We genotyped 1150 trees using 18 nuclear microsatellites and conducted population genetic analyses, including STRUCTURE, MIGRATE, BARRIER and Bayesian origin models. To investigate maternal phylogeography and infer lineage origins from a haplotype network, we analysed chloroplast single nucleotide polymorphisms.

Results: *A. marina* exhibited a strong genetic break between island populations (Seychelles, Aldabra, East Madagascar) and African mainland populations, reflecting Pleistocene divergence in nuclear and chloroplast markers. East African populations showed high genetic diversity, aligning with the northward flow of the bifurcated South Equatorial Current carrying limited traces of Late Pleistocene colonisation events. Ocean currents around Madagascar and eddie in the Mozambique Channel Area (MCA) facilitated long-distance dispersal since the Last Glacial Maximum, connecting islands like Mayotte and Europa. South-African range-edge populations showed low genetic diversity, likely due to limited dispersal and bottlenecks after the Late Holocene highstand. Aldabra populations displayed divergent haplotypes, suggesting multiple colonisation events.

Main Conclusions: Island populations (Seychelles, Aldabra, East Madagascar) experienced multiple Pleistocene colonisations, while mainland African and MCA populations were shaped by Holocene migration reflecting present-day ocean current patterns. Our findings help in better understanding the spatial patterns of genetic diversity and provide valuable insights for defining evolutionary significant and conservation units in the Western Indian Ocean.

Ludwig Triest and Tom Van der Stocken contributed equally to this paper.

1 | Introduction

Reconstructing the phylogeography of a species provides insights into the spatial and temporal variation in genetic diversity (Avise 2000). Genetic diversity enhances a species' ability to adapt to changing environmental conditions and is essential for long-term population viability (Frankham 2005). Patterns in genetic diversity are shaped by past colonisation events, range expansion and contraction in response to environmental changes, and barriers to gene flow (Hewitt 2000). Colonisation history influences the structure of genetic diversity, often leaving signatures of bottlenecks, founder effects, or secondary contact zones (Excoffier and Ray 2008; Taberlet et al. 1998). Phylogeographic analyses allow for the identification of Evolutionarily Significant Units (ESUs), which reflect populations with distinct evolutionary trajectories and potential local adaptations (Moritz 1994) and contribute to conservation and management strategies that preserve evolutionary potential and maintain biodiversity at the infraspecific level (Fraser and Bernatchez 2001).

Mangroves are coastal plants that inhabit intertidal areas at tropical, subtropical and some warm-temperate latitudes (Spalding et al. 2010), providing ecosystem services (Lee et al. 2014) including coastal flood protection (Hu et al. 2025), fishery production (Zu Ermgassen et al. 2025), and carbon sequestration (Donato et al. 2011). They are a polyphyletic group of ~70 species, with multiple taxa having independently invaded intertidal zones over the past ~50 Myr (He et al. 2022) and their constituent species having evolved adaptations to cope with the fluctuating conditions of intertidal habitats (e.g., changes in oxygen, moisture, temperature, salinity, and wave action) (Madhavan et al. 2025). Hydrochorous propagules are the primary mode of dispersal in mangroves. Positively buoyant propagules can be transported by riverine currents, tides, waves, surface ocean currents and influenced by wind (Van der Stocken et al. 2013), over local to transoceanic scales (Van der Stocken et al. 2019). Propagule dispersal plays a key role in maintaining genetic diversity, tracking suitable environmental conditions, and colonising new habitats, thereby determining the biogeography of species and the genetic diversity and structure of populations (Triest 2008). Despite their recognised importance and international conservation policies, global mangrove cover has declined due to deforestation for aquaculture, agriculture, and urban development, with more than 50% of the world's mangrove ecosystems classified as vulnerable, endangered, or critically endangered (IUCN 2024). Conversion to aquaculture, oil palm plantations, and rice cultivation explains 43% of mangrove losses between 2000 and 2020 (Leal and Spalding 2024). Besides impacts from human activities, mangroves are also threatened by the effects of climate change, including sea-level rise and increased exposure to severe weather events (Hülsen et al. 2025).

Avicennia L. is a widespread mangrove genus comprising eight currently recognised species distributed across two major biogeographic regions: *A. germinans*, *A. bicolor*, and *A. schaueriana* in the Atlantic–East Pacific (AEP); and *A. marina* (Forssk.) Vierh., *A. officinalis*, *A. alba*, *A. rumphiana*, and *A. integra* in the Indo–West Pacific (IWP) (Duke 1991). Molecular phylogenetic analyses (Li et al. 2016) and, more recently, a genome-wide phylogeny (He et al. 2022) revealed two well-supported monophyletic lineages corresponding to the AEP and IWP regions. Within the IWP, three robust subclades were identified: (1) *A. rumphiana* and *A. alba*, (2) *A. officinalis* and *A. integra*, and (3) the *A. marina* complex. These eight species remain recognised in the latest IUCN assessments (IUCN 2025) but may exhibit considerable geographic variation (Duke et al. 1998), introgressive hybridization (Mori et al. 2015), admixture, and signals of adaptive genetic differentiation (Sheidai et al. 2024). Species richness declines from the IWP towards the WIO, where *A. marina* is the sole representative (Wang et al. 2022). In the WIO, *A. marina* is found from the Red Sea to South Africa, across the Mozambique Channel Area (MCA), as well as coastal sites of Madagascar, the Seychelles and various small islands (Spalding et al. 2010). Strong genetic differentiation between East and South African *A. marina* populations, and high within-population inbreeding at the South-African latitudinal range limit has been linked to dispersal limitation due to the region's coastal geomorphology and range-edge effects (De Ryck et al. 2016). This raises questions about the role of MCA ocean circulation features in determining population connectivity between MCA coastal sites, including islands and atolls. Likewise, patterns of ancient and recent dispersal of *Rhizophora mucronata* in the WIO (Triest, Sierens, and Van der Stocken 2021) raise questions about the origin and connectivity of other mangrove species found across the WIO.

Population genetic data contributed to growing evidence of regional genetic connectivity and barriers to gene flow of *Avicennia* and *Rhizophora* in Southeast Asia (Do et al. 2019; He et al. 2019; Triest, Del Socorro, Gado, et al. 2021; Triest, Satyanarayana, Delange, et al. 2021; Triest, Van der Stocken, Sierens, et al. 2021; Triest et al. 2025; Wee et al. 2020), and the WIO (De Ryck et al. 2016; Triest, Sierens, and Van der Stocken 2021; Triest, Van der Stocken, De Ryck, et al. 2021). Large-scale studies across oceans that included WIO samples of *Bruguiera* (Urashi et al. 2013; Wee et al. 2014), *Rhizophora* (Lo et al. 2014; Takayama et al. 2021; Yan et al. 2016), *Xylocarpus* (Tomizawa et al. 2017), *Lumnitzera* (Manurung et al. 2023; Su et al. 2007) and *Heritiera* (Banerjee et al. 2020) have mostly focused on connectivity between the Eastern Indian Ocean (EIO) and the Western Pacific. Comprehensive WIO-wide genetic studies indicated the origins of multiple lineages and barriers to connectivity for *Rhizophora mucronata* (Triest, Sierens, and Van der Stocken 2021; Triest, Van der Stocken, De Ryck, et al. 2021). Barriers for mangrove dispersal include major landmasses (Wee et al. 2020), opposing ocean currents (Ngeve et al. 2016) and possibly upwelling (Ximenes et al. 2025). On smaller scales, factors like estuarine fragmentation (Binks et al. 2019), geomorphological features (Triest and Van der Stocken 2021), river outflows (Hasan et al. 2018), coastal channelling (Triest et al. 2020) and inland river-fringed habitats (De Ryck et al. 2016) affect connectivity. Hence, ocean-dispersed species are not necessarily panmictic (Gallaher et al. 2017; Maguire et al. 2000). While traces of Pleistocene dispersal events are hard to detect genetically, Holocene events have left clearer genetic signatures, forming admixed gradients in *Avicennia* or *Rhizophora* across the East Pacific (Sandoval-Castro et al. 2014), East Atlantic (Ngeve et al. 2016) and WIO (Triest, Sierens, and Van der Stocken 2021;

Triest, Van der Stocken, De Ryck, et al. 2021). Contrasting patterns from nuclear microsatellites and chloroplast sequence (cpDNA) data suggest distinct Pleistocene and Holocene long-distance dispersal (LDD) to the Seychelles and Madagascar in *R. mucronata* (Triest, Sierens, and Van der Stocken 2021). The scarcity of comprehensive palaeontological data and insights based on fossil and microfossil mangrove tree material (Srivastava and Prasad 2019) underscore the importance of molecular approaches (He et al. 2022). Chloroplast sequences may reveal evolutionary processes not detected by microsatellites alone, improving our understanding of fine-scale divergence. For example, cpDNA data have linked *Bruguiera gymnorhiza* populations in Madagascar with those in the EIO (Urashi et al. 2013) and revealed shared haplotypes of *Xylocarpus granatum* between the South China Sea and the WIO (Tomizawa et al. 2017).

Here, we conduct a large-scale population genetic study to reconstruct the colonisation history of *A. marina* in the WIO region. Our sampling strategy was informed by the region's large-scale surface ocean circulation patterns and included *A. marina* populations from across the WIO. Outgroups include peripheral Red Sea and distant Southeast Asia populations. We analysed spatial genetic diversity and structure using eighteen polymorphic nuclear microsatellite loci and nearly full chloroplast genomes.

2 | Materials and Methods

A detailed description of materials and methods is provided in Appendix S1.

2.1 | Study Area and Sampling

A total of 1150 individuals of *Avicennia marina* from natural mangrove forests were collected, specifically 1079 trees from 34 locations in the WIO (Table 1, Figure 1), of which 22 were located along the continental eastern African coastline from a northernmost site in Lamu, Kenya, to the southern range limit of the species at Wavecrest, South Africa. Twelve populations were located on Madagascar, Europa Island, Mayotte Island in the Comoros archipelago, Aldabra Atoll and Granitic Seychelles (Mahé and Curieuse Island, hereafter referred to as 'Seychelles'). As outgroup, we included 71 individual trees from the Red Sea (Saudi Arabia), the EIO (western Malaysian Peninsula), and the East Sea (northern Vietnam). For Next Generation Sequencing (NGS)-based chloroplast genome assembly, a subset of 50 individuals was used and included additional Southeast Asian provenances (Appendix S2, Table S2.1).

2.2 | Microsatellite Analysis and Data Quality

DNA extractions, PCR conditions, and data quality checks followed methods as described in Triest et al. (2025). We used 18 microsatellite loci assembled in two multiplex sets. A quality check was performed regarding large allele dropout, linkage disequilibrium, null alleles, and power to discriminate individual *A. marina* trees.

2.2.1 | Allelic and Genetic Diversity of Individuals and Populations

The effective number of alleles (A_E), observed heterozygosity (H_O) and unbiased heterozygosity (uH_E) were calculated using GENALEX v6.502 (Peakall and Smouse 2012), whereas the total number of alleles (A_T), allelic richness (A_R) for a minimum threshold of 12 diploid individuals ($k = 24$), and the within-population inbreeding coefficient (F_{IS}) were calculated using FSTAT v2.9.3.2 (Goudet 2001). A population assignment test (option 'leave-one-out') and estimation of the number of private alleles and their frequencies (q) were done in GENALEX. The selfing rate (S) was estimated assuming a mixed mating model using SPAGEDI v1.5a (Hardy and Vekemans 2002). To detect recent genetic bottlenecks in populations, Wilcoxon sign-rank tests were performed in BOTTLENECK v1.2.02 (Piry et al. 1999).

2.2.2 | Indirect Estimations of Connectivity

To identify clusters of individuals and populations at WIO level, a Principal Coordinate Analysis (PCoA) of individual codominant genotypes and of mean population differentiation (F_{ST}) was used in GENALEX. Pairwise genetic differentiation of populations (F_{ST}) and their overall structure among populations (F_{ST}), within individuals (F_{IS}), and among individuals (F_{IT}) was calculated via AMOVA-F_{ST} with 999 permutations at population level within the WIO ($N = 34$), within two regions (western WIO, $N = 28$; eastern WIO, $N = 6$), and hierarchically (F_{RT}) between these regions. Pairwise F_{ST} values were used in a Mantel test.

2.2.3 | Evolutionary Signal Over Geographical Distance

To estimate the overall evolutionary signal from allele size differences, microsatellite-based R_{ST} values are expected to exceed F_{ST} values. An ANOVA approach (1-sided test, 1000 randomizations) was used to test for significance of lower differentiation (F_{ST} or R_{ST}) at short distances and significance of higher differentiation levels (F_{ST} or R_{ST}) over longest geographical distances using SPAGEDI.

2.2.4 | Genetic Structure and Barrier Analysis

To determine gene pools, a Bayesian clustering analysis of individuals was carried out in STRUCTURE v2.3.4 (Pritchard et al. 2000). The admixture model ran 10 iterations for each K value from 1 to 40; the burn-in period was 50,000 with 500,000 Markov chain Monte Carlo repeats. To detect sharp genetic changes between neighbouring populations, we considered pairwise F_{ST} matrices of 18 microsatellite loci and an overall pairwise F_{ST} matrix, allowing two barriers per matrix, using BARRIER v2.2 (Manni et al. 2004).

2.2.5 | Directionality of Historical Gene Flow

Specific hypotheses on migration directionality were tested using panmixia, stepping-stone (bi- and unidirectional) or

TABLE 1 | Geographic location, sample size and genetic diversity variables of 34 populations of *Avicennia marina* of the Western Indian Ocean. Population codes are as in Figure 1.

Region/country locality	Code	N	G	A_T	A_E	A_R	H_O	uH_E	F_{IS}	S	Bottle-neck	Gene pool	Haplo group	Latitude	Longitude
African mainland															
Kenya															
Lamu Island	KEN1	21	21	63	2.1	3.2	0.375	0.434	0.140	0	ns	GP1	HG2	−2.256219	40.895858
Mida Creek	KEN2	39	39	83	2.4	3.6	0.412	0.494	0.167*	0.14*	ns	GP1	HG1	−3.374781	39.959842
Gazi Bay	KEN3	34	34	64	2.1	3.0	0.402	0.415	0.033	0	ns	GP1	HG1,2	−4.422058	39.513361
Vanga	KEN4	51	51	70	2.2	3.1	0.424	0.435	0.025	0.08*	ns	GP1	HG1	−4.654264	39.220467
Tanzania															
Pemba	TAN1	30	30	53	1.6	2.5	0.258	0.314	0.180*	0	ns	GP1	HG1	−4.982758	39.702836
Mbweni	TAN2	29	29	46	1.9	2.4	0.312	0.372	0.163	0.19*	ns	GP1	HG1	−6.631550	39.188467
Mafia	TAN3	25	25	44	1.8	2.4	0.238	0.348	0.321*	0.57***	ns	GP1	HG1	−7.967281	39.748253
Mtwara	TAN4	30	30	54	1.9	2.6	0.256	0.307	0.168*	0.20*	***	GP1	HG1	−10.289039	40.214492
Mozambique															
Pemba	MOZ1	31	31	63	1.9	2.9	0.256	0.331	0.229*	0.06	*	GP2	HG1	−12.972547	40.517075
Nacala	MOZ2	35	35	57	1.8	2.7	0.265	0.323	0.184*	0.08	*	GP2	HG1	−15.006947	40.770689
Quelimane	MOZ3	31	30	69	2.3	3.2	0.355	0.382	0.071	0.13*	ns	GP2	HG1	−17.876442	36.866064
Vilanculos	MOZ4	19	19	43	1.8	2.2	0.245	0.294	0.171	0.24	ns	GP2	HG1	−22.014939	35.322014
Dambula	MOZ5	17	17	50	1.9	2.7	0.291	0.367	0.212*	0	ns	GP2	HG1	−22.208389	35.399183
Mahoa	MOZ6	27	27	47	1.6	2.3	0.290	0.322	0.100	0.18*	***	GP2	HG1	−22.157550	35.441303
Barra	MOZ7	35	35	48	1.6	2.3	0.256	0.287	0.109	0.08	ns	GP2	HG1	−23.795700	35.499400
Limpopo	MOZ8	38	38	51	1.7	2.4	0.257	0.285	0.099	0.20**	ns	GP2	HG1	−25.163300	33.505800
Inhaca	MOZ9	32	32	43	1.7	2.2	0.219	0.254	0.41	0.15	ns	GP2	HG1	−26.038100	32.902800
South Africa															
St. Lucia	SAF1	32	14	34	1.1	1.6	0.040	0.092	0.572*	0.79***	ns	GP3	HG1	−28.380800	32.421700
Mlalazi	SAF2	29	22	25	1.2	1.3	0.042	0.116	0.642*	0.29	**	GP3	HG1	−28.954900	31.775300
Mgeni	SAF3	33	32	42	1.5	2.0	0.152	0.245	0.386*	0.21	ns	GP3	HG1	−29.808700	31.040000
Mngazana	SAF4	39	38	43	1.5	2.1	0.134	0.225	0.408*	0.21	***	GP3	HG1	−31.692900	29.413900
Wavecrest	SAF5	47	25	25	1.2	1.4	0.035	0.091	0.624*	0.81*	*	GP3	HG1	−32.580700	28.523600

(Continues)

TABLE 1 | (Continued)

Region/country locality	Code	N	G	A_T	A_E	A_R	H_O	uH_E	F_{IS}	S	Bottle-neck	Gene pool	Haplo group	Latitude	Longitude
Mozambique Channel Islands and Madagascar															
Comoros Islands															
Mayotte	MAY	60	59	56	1.7	2.3	0.262	0.302	0.134*	0.13*	ns	GP1 + 2	HG4	−12.921200	45.150911
Europe Island															
Europe	EUR	30	30	53	1.6	2.4	0.189	0.233	0.190*	0	***	GP2	HG1	−22.361822	40.386314
Madagascar															
Ramena	MAD1	31	30	52	1.8	2.5	0.296	0.342	0.137	0.01	ns	GP2	HG1	−12.257517	49.342033
Andilana	MAD2	29	28	44	1.6	2.2	0.188	0.263	0.288*	0.09	ns	GP2	HG1	−13.252631	48.181728
Morondova	MAD3	34	33	56	1.8	2.6	0.258	0.283	0.089	0.17*	ns	GP2	HG1	−20.296725	44.267478
Sarodrano	MAD4	20	20	43	1.6	—	0.201	0.293	0.334*	0.57***	**	GP2	HG1	−23.530306	43.741914
Foulpointe	MAD5	29	20	35	1.2	1.7	0.039	0.094	0.594*	0	ns	GP4	HG4	−17.682436	49.516303
Seychelles Islands															
Aldabra Atoll															
La Gigi	ALD1	30	29	33	1.3	—	0.097	0.160	0.400*	0.33	*	GP4	HG4	−9.403491667	46.20967778
Ile Michel	ALD2	30	30	36	1.4	—	0.230	0.227	−0.016	0	ns	GP4	HG5	−9.400247222	46.44819722
Granitic Seychelles															
Mahé Island—Ile du Port	SEY1	26	8	21	1.0	—	0.013	0.036	0.651*	—	***	GP5	HG5	−4.613261	55.458731
Mahé Island—Grand Anse	SEY2	29	16	18	1.0	—	0.032	0.041	0.222	0.48	***	GP5	HG5	−4.682269	55.452181
Curieuse Island	SEY3	27	6	20	1.0	—	0.006	0.018	0.659*	—	***	GP5	HG5	−4.285486	55.727808
Outgroup															
Ras Masturah, Saudi Arabia, Red Sea	SAR	8	8	48	1.9	—	0.299	0.338	0.125	0.31*	*	NA	HG3	23.108455	38.808359
Matang, Malaysia P., Andaman Sea	MAL	33	33	52	1.7	—	0.141	0.277	0.496*	—	ns	NA	NA	4.85890	100.55670
Tam Giang, Vietnam, East Sea (SCS)	VIE	30	30	39	1.5	—	0.176	0.234	0.253*	—	*	NA	NA	15.47310	108.65440

Note: Additional populations beyond the WIO region and considered as outgroup for several microsatellite data analysis (PCoA, STRUCTURE, DIYABC).
Abbreviations: A_E, effective number of alleles; A_R, allelic richness at $k = 24$; A_T, total number of alleles; F_{IS}, within-population inbreeding; G, number of unique genotypes; H_O, observed heterozygosity; N, number of samples; NA, not applicable as outgroup; ns, non-significant; S, selfing rate; uH_E, unbiased expected heterozygosity.
*$p < 0.05$.
**$p < 0.01$.
***$p < 0.001$.

source-sink models for migration of *A. marina* populations for (1) East African sites and hypothesis of divergence from MCA through the East African Coastal Current (EACC); (2) MCA sites and hypothesis of a split through the dominant southward flow field of propagating anticyclones; (3) West Madagascar sites and hypothesis of the Southwest Madagascar Coastal Current (SMCC); (4) Connectivity of Mayotte Island and (5) Europa Island with Madagascar and African main coast across the MCA. MIGRATE-N (Beerli 2006; Beerli and Palczewski 2010) was used as outlined in Triest et al. (2025).

2.2.6 | Phylogeography and Origin Models of Microsatellite-Based Gene Pools

To estimate the origin and time of divergence of *A. marina* from different WIO regions, we considered five microsatellite gene pools using the approximate Bayesian computation (ABC) approach implemented in DIYABC-RF v1.0 (Collin et al. 2021) and compared nine scenarios (Appendix S3, Figure S3.1). Priors of generation times were 100,000 for t_d, 75,000 for t_1, 50,000 for t_2, 25,000 for t_3, and 10,000 for t_4. *Ne* population size prior was set to 10,000. The most supported scenario was used for estimation of divergence times (as generations) t_d, t_1, t_2, t_3, t_4 and effective population sizes of the ancestral population Ne_A and each of the five present-day gene pools GP1 to GP5 (as Ne_1 to Ne_5). Summary statistics, noise variables and goodness of fit were considered as in Triest et al. (2025). The generation time of *Avicennia*, i.e., the average interval between the formation of an individual propagule and the production of its offspring was considered 3 to 5 years when converting t generations into years as implemented by Ochoa-Zavala et al. (2019) and further argued in Triest et al. (2025).

2.3 | Chloroplast Mutations, ML Tree, Haplogroups and Origin Models

The analysis of complete chloroplast sequences through genome skimming followed protocols as mentioned in Triest et al. (2025). All mutational steps were recorded; however, we omitted interference from nuclear copies of plastid DNA (NUPTs) in 33 genes of the Large Single Copy (LSC) region and retained only mutational differences from non-ambiguous sequences for alignment and further analysis.

To present phylogenetic relationships of maternal lineages of *A. marina* in the WIO, relative to the outgroups, a Maximum Likelihood (ML) tree using all mutations was constructed with MRBAYES 3.2.6 (Huelsenbeck and Ronquist 2001). A median-joining network (Bandelt et al. 1999) using POPART v1.7.2 (Leigh and Bryant 2015) served for haplotype network construction and haplogroup definition.

To estimate the maternal origin and divergence time of *A. marina* of different WIO regions, we considered five WIO haplogroups (not exactly corresponding to the five microsatellite gene pools) in ABC origin models in DIYABC-RANDOMFOREST using nine scenarios and priors as in 2.2.6 (Appendix S4, Figure S4.1).

3 | Results

3.1 | Allele Diversity and Bottlenecks

A total of 167 alleles across 18 microsatellite loci were identified in 1150 individuals, revealing 1029 unique multilocus genotypes (MLGs). Repeated MLGs were mainly found in South Africa, East Madagascar, and the Seychelles. Along the African mainland coast, the number of alleles ranged from 29 to 83, with allelic richness from 1.3 to 3.6 (Table 1). Among island populations, allele counts ranged from complete monomorphism across all 18 loci to 56, with effective allele numbers (A_E) ranging from 1 in the Seychelles to 1.8 in Madagascar (Table 1). A general decline in allele diversity was observed along a north-to-south gradient from continental Africa. Allele distribution was highly uneven on Madagascar and nearby islands. Diversity was highest in northern and western Madagascar, Mayotte, and Europa, but sharply reduced along East Madagascar, Aldabra, and the Seychelles (Table 1).

Kenyan and Tanzanian populations formed an allelic diversity hotspot, while remote islands of Aldabra—and especially the Seychelles—had fewer but unique allele variants. Regionally, Aldabra and the Seychelles contained 10 private alleles with a relatively high mean frequency (^q = 0.169). In contrast, 80 private alleles were found at low frequencies elsewhere (^q = 0.041), often detected once and typically in heterozygous individuals. *Avicennia marina* populations on smaller islands varied considerably in allele number per locus. Mayotte, Europa, and Aldabra populations had more than two alleles at several loci, suggesting either multiple colonisation events or local accumulation of stepwise mutations. In contrast, all three Seychelles sites exhibited only one or two alleles per locus, indicating either a single founder origin or severe population bottlenecks. A BOTTLENECK analysis revealed that seven populations experienced significant recent bottlenecks ($p < 0.001$), including all Seychelles populations, Europa Island, and several mainland African sites (Table 1).

3.2 | Gene Diversity and Local Inbreeding

The highest heterozygosity levels (H_O and uH_E; Table 1), consistent with patterns of allelic richness, were found in populations from Kenya, Tanzania and Mozambique. In contrast, the lowest heterozygosity levels occurred in South Africa, East Madagascar, one Aldabra site (ALD1), and across the Seychelles. Within-population inbreeding (F_{IS}) was significant in 20 of 34 populations, with values ranging from 0.167 to 0.659 (Table 1). No significant inbreeding (non-significant F_{IS}) was observed in 15 populations, mainly along East African and MCA coastlines, and at one Aldabra site (ALD2). The estimated selfing rate (S) was significant and high (0.13–0.81) in 14 populations, though large standard errors suggest mixed mating systems (Table 1).

Pairwise genetic differentiation (F_{ST}) within regions (Figure 2A) was highest among the 'eastern' WIO populations—MAD5, Aldabra and the Seychelles—with values ranging from F_{ST} = 0.407 to 0.935 (Table S2.2). These levels were nearly as high as those observed for outgroup populations in the Red Sea,

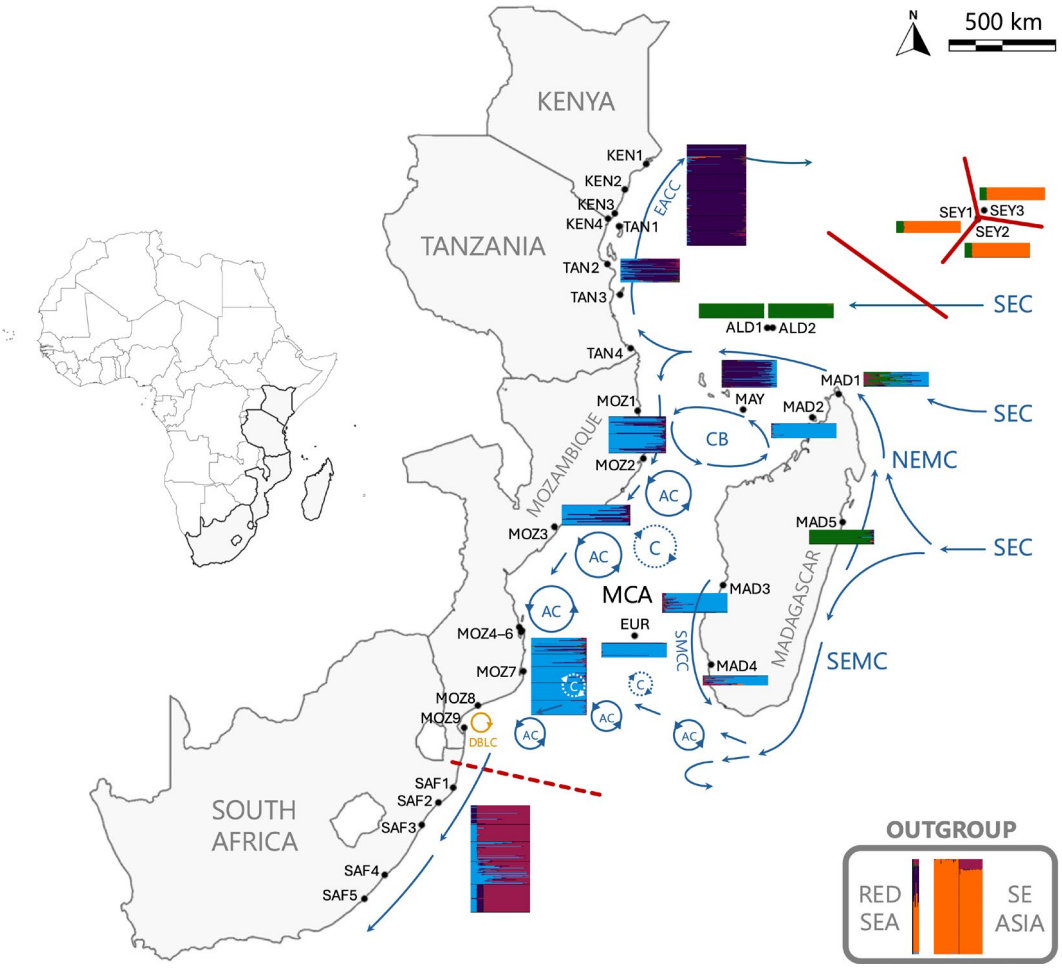

FIGURE 1 | Location of 34 *Avicennia marina* sites in the Western Indian Ocean. Population codes are as in Table 1. Bar charts per population or region summarise the genetic structure inferred by STRUCTURE analysis ($K = 5$ including an outgroup). Red lines indicate a major (full) or minor (dashed) break from a BARRIER analysis. Main ocean surface current directionality is indicated with blue arrows (adapted from Hancke et al. 2014). AC: Anticyclonic eddies; C: Cyclonic eddies; CB: Comoros Basin; DBLC: Delagoa Bight Limpopo Current; EACC: East African Coastal Current; MCA: Mozambique Channel Area; NEMC: Northern Equatorial Madagascar Current; SEC: South Equatorial Current; SEMC: Southern Equatorial Madagascar Current; SMCC: Southwest Madagascar Coastal current.

Malaysia, and Vietnam. In contrast, the 'western' WIO populations along the main African coast, including MCA sites of Mayotte, Europa, and western Madagascar, showed much lower F_{ST} values, ranging from 0.053 to 0.300, except for a few inbred South African populations. All pairwise F_{ST} values were statistically significant ($p < 0.001$).

3.3 | Genetic Structure of *A. marina* Populations

A PCoA of individuals from the WIO showed a clear separation along the first axis between the Seychelles and Aldabra Atoll from other populations, whereas East Madagascar separated from West Madagascar along a third axis (Figure 3A). Although individuals from the 'western' WIO region overlapped substantially, a north–south gradient appeared along the third axis. Individuals largely clustered with others from the same population, indicating strong population-level genetic differentiation (Figure 3A). An assignment test confirmed this, with 88% of individuals correctly assigned to their source population and only 12% assigned to a different one, mostly within East Africa. A PCoA of 34 WIO populations and 3 outgroup populations (Figure S2.1) also showed clear separation: the outgroup and eastern WIO populations were distinct along the first axis, while the WIO populations were separated from the Red Sea and Southeast Asian outgroups along the second axis. As with the individual-level PCoA, populations from the Seychelles, Aldabra, and East Madagascar were clearly distinct from those in the western WIO.

STRUCTURE analysis identified the highest Delta$K$ at $K = 2$, indicating two main genetic clusters. The first cluster comprised a widespread 'western WIO' group, including all populations from Kenya, Tanzania, Mozambique, South Africa, northern and western Madagascar, Europa Island, and Mayotte (Figures 1 and S2.2). The second cluster represented an 'eastern WIO' group, encompassing East Madagascar, Aldabra Atoll, the Seychelles, and the outgroup populations from the Red Sea, Malaysia, and Vietnam. While $K = 2$ captures the broadest division, the WIO likely harbours more than two gene pools. Clusters from $K = 2$ to $K = 5$ formed relatively homogeneous regional blocks with a low standard deviation in ln$P(K)$, suggesting biologically meaningful structure. From $K = 6$ onward, additional clusters mostly represented admixed individuals with low assignment values (Q), which

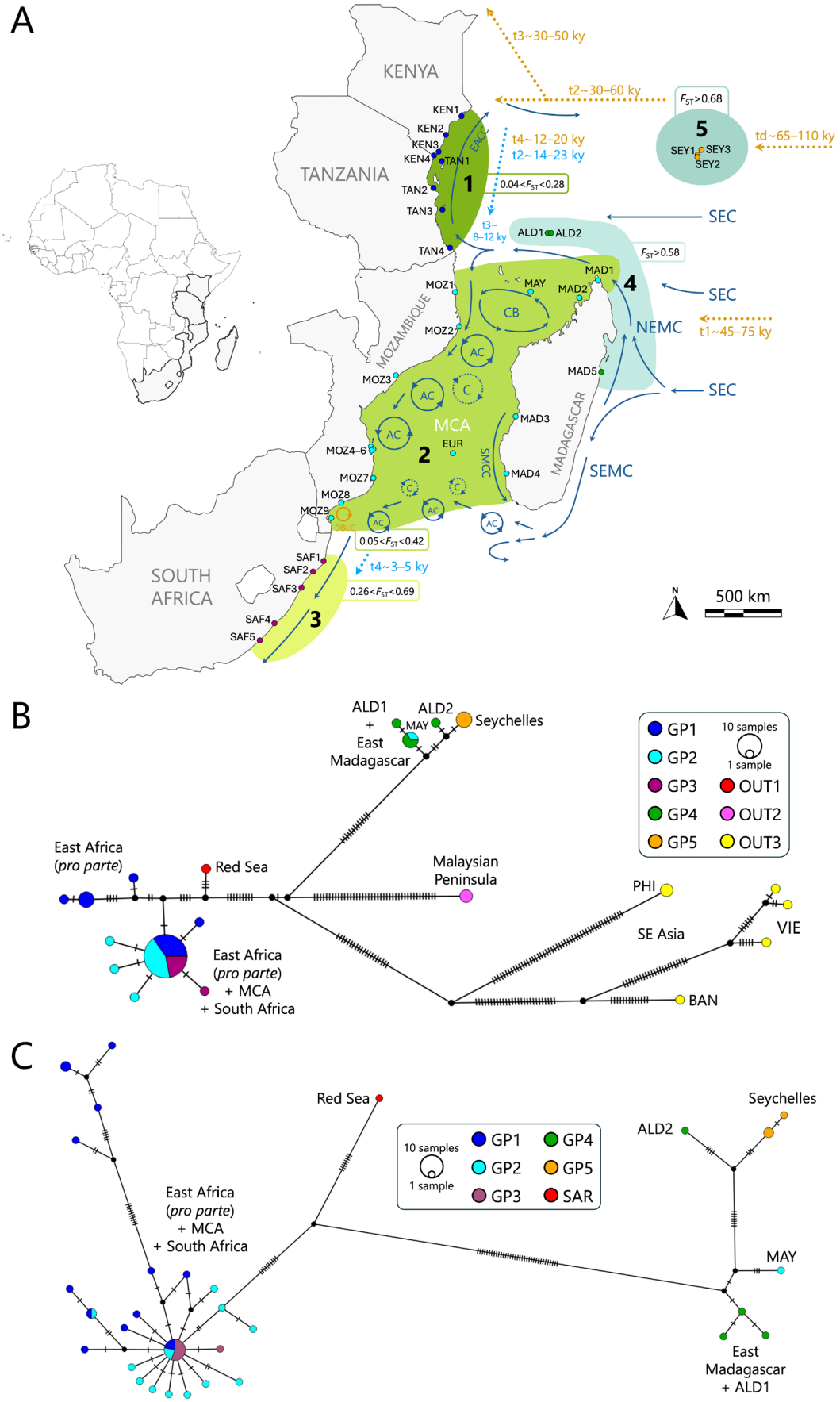

FIGURE 2 | Legend on next page.

FIGURE 2 | Genetic grouping of *Avicennia marina* populations with (A) five gene pools based on microsatellite data. Green and blue colours of five groups indicate the major genetic break of eastern and western Evolutionary Significant Units in the WIO (STRUCTURE analysis $K = 2$). F_{ST} ranges within each gene pool are provided with highest values for gene pools 4 and 5. The times of divergence (t_2, t_3, t_4 in blue) are from an origin model based on microsatellites and times of divergences (t_d, t_1, t_2, t_3, t_4 in orange) are from an origin model based on chloroplast haplotypes. Major ocean surface current directions are similar to Figure 1. (B) Chloroplast haplotype network of mutational substitutions (transitions and transversions) in the WIO, Red Sea, relative to an extended Asian outgroup. Note a similar mutational number of Red Sea and East Africa (pro parte) from their nearest shared node; (C) Chloroplast haplotype network of all mutations (transitions, transversions, mononucleotide repeats and insertion/deletions) in the WIO and Red Sea, indicating the eastern WIO populations (Seychelles, Aldabra, East Madagascar) as an evolutionary unit. The numbers of lines between haplotypes indicate the position of the corresponding mutations in the alignment. Colours in both haplotype networks refer to the five gene pools and outgroup, as given by nuclear microsatellites.

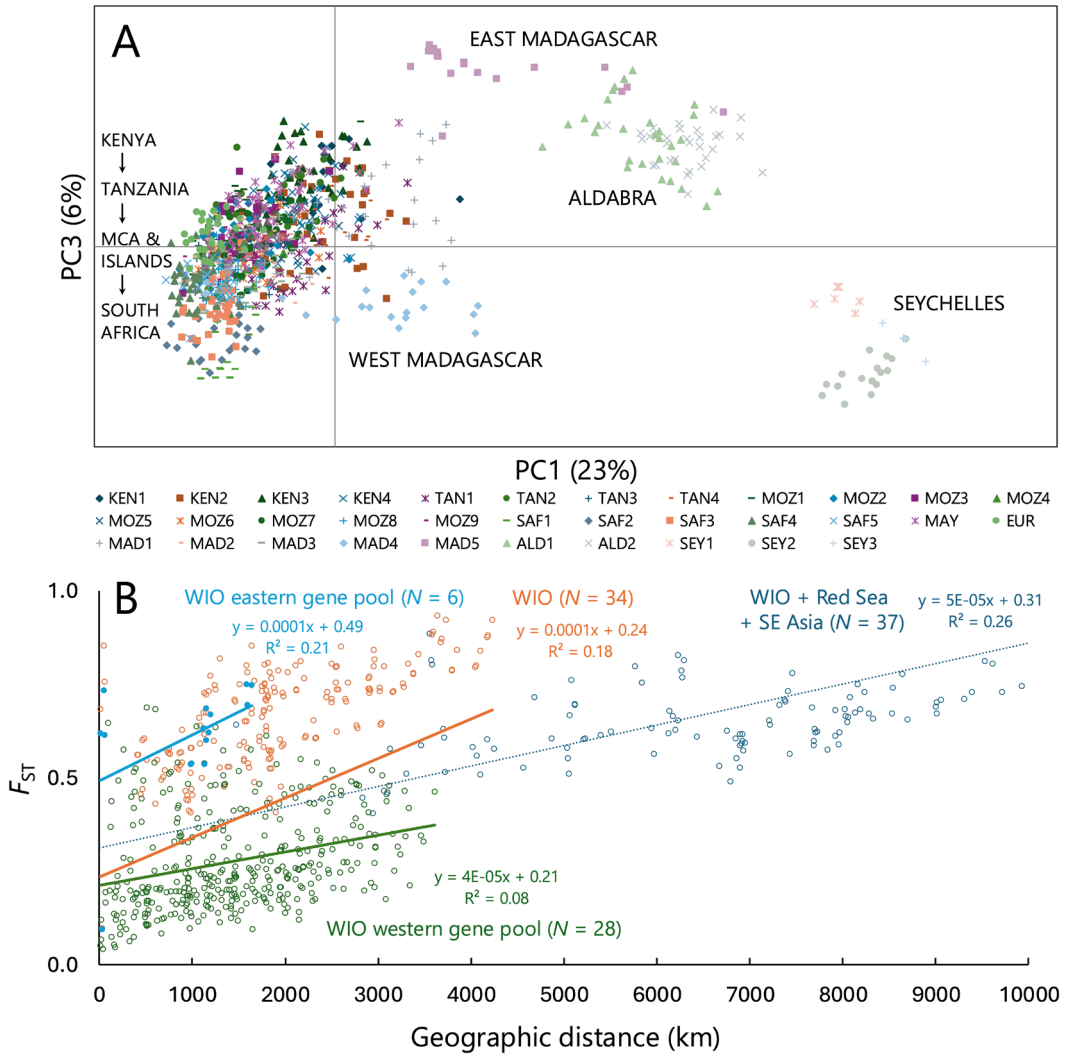

FIGURE 3 | (A) PCoA of individual *Avicennia marina* genotypic distances from nuclear microsatellites in major regions and islands of the WIO, clearly separating the eastern WIO islands from a main western WIO cluster that contains a latitudinal gradient. (B) Isolation-by-distance (IBD) with geographic distance (km) as an explanatory factor of F_{ST} between populations for four data sets, namely WIO including Southeast Asian outgroup (blue), WIO (orange) and the eastern WIO gene pool (blue) showing strongest IBD slope when compared to the western gene pool (green).

are potentially informative for assessing regional connectivity (Figure S2.2). Based on this, five gene pools (GP) could be considered (Table 1), namely GP1: East Africa; GP2: MCA; GP3: South Africa; GP4: East Madagascar and Aldabra; and GP5: Seychelles, Red Sea, and Southeast Asian outgroups. Admixture patterns from GP2 to GP1 were also observed near the SEC bifurcation and on Mayotte Island, whereas northern Madagascar showed mixed ancestry from GP2 and GP4 (Figures 1 and S2.2). These five gene pools were significantly different for standard genetic variables (Table S2.3).

3.4 | Barriers and Strongest Differences

BARRIER analysis revealed major genetic breaks separating the Seychelles, Aldabra Atoll, and East Madagascar from other

TABLE 2 | Summary of AMOVA and *F*-statistics of *Avicennia marina* for all populations and a hierarchical AMOVA considering two regions, that account for the largest variance of the Western Indian Ocean populations, namely the eastern WIO (Seychelles, Aldabra and East Madagascar) as an eastern ancient group versus all other African and West Madagascar populations.

	df	SS	MS	Est. Var.	%	*F*-statistics	*p*
No regions							
Among populations	33	4,394,282	133,160	2052	44%	$F_{ST}=0.444$	0.001
Among individuals	1045	3,350,212	3206	0,637	14%	$F_{IS}=0.248$	0.001
Within individuals	1079	2,085,000	1932	1932	42%	$F_{IT}=0.582$	0.001
Total	2157	9,829,494		4621	100%	$Nm=0.3$	
Two regions							
Among regions	1	1,507,708	1,507,708	2473	39%	$F_{RT}=0.386$	0.001
Among populations	32	2,886,574	90,205	1371	21%	$F_{SR}=0.348$	0.001
Among individuals	1045	3,350,212	3206	0,637	10%	$F_{ST}=0.599$	0.001
Within individuals	1079	2,085,000	1932	1932	30%	$F_{IS}=0.248$	0.001
Total	2157	9,829,494		6413	100%	$F_{IT}=0.699$	0.001

Abbreviations: df, degrees of freedom; Est. Var., estimated variance; MS, mean of squares; SS, sum of squares.

populations (Figures 1 and S2.3). Minor barriers among South African populations reflect elevated inbreeding levels due to isolation from neighbouring mangroves, whereas minor genetic barriers in East Africa might arise from their unique and higher diversity levels (See further under 3.7). Overall genetic differentiation among WIO populations was high (AMOVA-$F_{ST}=0.444$; Table 2). Most of this differentiation occurred between the eastern and western WIO regions (hierarchical AMOVA-$F_{RT}=0.386$). Notably, the six eastern WIO populations showed much higher differentiation (AMOVA-$F_{ST}=0.698$) compared to the 28 western WIO populations (AMOVA-$F_{ST}=0.275$; Table S2.4).

3.5 | Isolation-By-Distance Testing

Four Mantel tests—covering all 37 populations (including outgroups), 34 WIO populations, and each $K=2$ group ($N=28$ and $N=6$) – showed the strongest IBD in the Seychelles and Aldabra populations, and the weakest IBD among African mainland and MCA populations (Figure 3B). An ANOVA over ten geographic distance classes for the 34 WIO populations (Table S2.5) revealed significantly lower genetic differentiation (F_{ST} and R_{ST}) at short distances (<1453 km) compared to the average (mean pairwise $F_{ST}=0.448$; $R_{ST}=0.520$). Conversely, a significant IBD effect was detected at largest distances (>2500 km) for both F_{ST} and R_{ST}. The overall IBD slope was significant for F_{ST} ($b=0.088$, $p<0.001$) and R_{ST} ($b=0.091$, $p<0.001$). Similar analyses within the $K=2$ groups showed significant IBD beyond 2667 km in the western WIO, but not in the eastern WIO, where a genetic break was observed instead (Table S2.5).

3.6 | Migration Models

Migration models for *A. marina* (Table 3) focused on the most closely related populations with the lowest F_{ST} from gene pools GP1 and GP2. These included: (a) East African sites (GP1), showing northward flow along the bifurcated SEC via the EACC; (b) MCA sites (GP2), following a southward bifurcated SEC; (c) West Madagascar sites (GP2), influenced by the SMCC; (d) Mayotte Island (GP2 but admixed with GP1), indicating connectivity across the MCA with northern Madagascar (GP2) and the nearby African mainland; and (e) Europa Island (GP2), showing potential links to nearby Madagascar and the African mainland. Testing directionality across mangrove estuaries revealed that customised stepping-stone models were more likely than panmixia, bidirectional stepping-stone, or various source-sink models, except for the MCA islands (Table 3).

3.7 | Origin Models of Five Microsatellite-Based Gene Pools

Among nine tested origin scenarios (Appendix S3, Figure S3.1) and demographic evolution of *A. marina* gene pools GP1 to GP5 in the WIO—based on a Southeast Asian ancestral outgroup at time t_d—phylogeographic scenario 6 (Figures 4B and S3.2) was best supported (30% votes, 0.43 probability). This scenario identifies GP5 (Seychelles) as the oldest WIO lineage followed by GP4 (East Madagascar, Aldabra), then GP1 (East Africa), GP2 (MCA), and finally GP3 (South Africa). Estimated median generations ranged from $t_4=935$ for the youngest South African lineage to $t_d=15{,}452$ for the ancestral root (Table 4; Figures 4B and S3.3). Assuming a generation time of 5 years (Table 4), the divergence of GP5 and GP4 (Seychelles, Aldabra and East Madagascar) dates to 40,818–77,260 years ago, corresponding to the Late Pleistocene. GP1 (East Africa, including admixed Mayotte) diverged near the end of the LGM (~23,320 years ago), while GP2 (MCA) and the most recent GP3 (South Africa) diverged during the Holocene around 11,985 and 4675 years ago, respectively. Effective population sizes were highest in ancestral populations, outgroup GP4 and GP5 ranging from 4249 to 6413. In contrast, recent populations GP1, GP2 and GP3 had lower *Ne*

TABLE 3 | Comparison of migration models on the directionality of *Avicennia marina* populations in the WIO. Migration models were simulated for (a) East African sites and testing hypothesis of split SEC into northward direction East African Coastal Current (EACC); (b) Mozambican channel sites and hypothesis of split SEC into southward direction; (c) West Madagascar sites and hypothesis of the Southwest Madagascar Coastal Current (SMCC); (d) Connectivity of Mayotte Island with Madagascar and African main coast across the Mozambique Channel Area; (e) Connectivity of Europa Island with Madagascar and African main coast across the Mozambique Channel Area.

Geographical region	Model	Directionality	Connected populations (minimum and maximum km distance between pairs)	Bezier log marginal-likelihood	C	P
a. **East Africa (Northward split of SEC)**			Eight mangrove areas (47–263 km)			
	Panmixia	All	All	−761,495.28	4	0
	Stepping-stone	Bidirectional	KEN1 ← → KEN2 ← →KEN3 ← → KEN4 ← → TAN1 ← → TAN2 ← →TAN3 ← → TAN4	−287,858.87	3	0
	Stepping-stone	Unidirectional from North to South	KEN1 → KEN2 →KEN3 → KEN4 → TAN1 → TAN2 →TAN3 → TAN4	−77,133.16	2	0
	Stepping-stone	Unidirectional from South to North	KEN1 ← KEN2 ← KEN3 ← KEN4 ← TAN1 ← TAN2 ← TAN3 ← TAN4	−75,290.99	1	1
(b) Mozambique (Southward split of SEC)			Eight mangrove areas (7–525 km)			
	Panmixia	All	All	−613,969.53	4	0
	Stepping-stone	Bidirectional	MOZ1 ← → MOZ2 ← → MOZ3 ← → MOZ4 ← → MOZ5 ← → MOZ6 ← → MOZ7 ← → MOZ8	−326,981.81	3	0
	Stepping-stone	Unidirectional from North to South	MOZ1 → MOZ2 → MOZ3 → MOZ4 → MOZ5 → MOZ6 → MOZ7 → MOZ8	−91,382.64	1	1
	Stepping-stone	Unidirectional from South to North	MOZ1 ← MOZ2 ← MOZ3 ← MOZ4 ← MOZ5 ← MOZ6 ← MOZ7 ← MOZ8	−114,925.25	2	0
(c) West Madagascar (Southwest Madagascar Coastal Current)			Four mangrove areas (168–887 km)			
	Panmixia	All	All	−587,036.93	4	0
	Stepping-stone	Bidirectional	MAD1 ← → MAD2 ← → MAD3 ← → MAD4	−482,781.30	3	0
	Stepping-stone	Unidirectional from North to South	MAD1 → MAD2 → MAD3 → MAD4	−232,579.94	1	1
	Stepping-stone	Unidirectional from South to North	MAD1 ← MAD2 ← MAD3 ← MAD4	−265,038.59	2	0

(Continues)

TABLE 3 | (Continued)

Geographical region	Model	Directionality	Connected populations (minimum and maximum km distance between pairs)	Bezier log marginal-likelihood	C	P
(d) Mayotte Island (MCA Eddies)			Remote island (460–526 km)			
	Panmixia	All	All	−732,448.04	5	0
	Source-Sink	Madagascar as source for island and mainland	MAY ← MAD1 MOZ2 ← MAD1	−712,678.14	4	
	Source-Sink	Mayotte island as sink of Madagascar and source for mainland	MOZ2 ← → MAY ← MAD1	−449,423.40	1	
	Stepping-stone	Bidirectional	MOZ2 ← → MAY ← → MAD1	−747,799.87	6	0
	Stepping-stone	Unidirectional from West to East	MOZ2 → MAY → MAD1	−475,439.26	3	0
	Stepping-stone	Unidirectional from East to West	MOZ2 ← MAY ← MAD1	−473,611.20	2	1
(e) Europe Island (MCA Eddies)			Remote island (463–509 km)			
	Panmixia	All	All	−575,456.67	5	0
	Source-Sink	Madagascar as source for island and mainland	EUR ← MAD3 MOZ6 ← MAD3	−592,307.37	6	0
	Source-Sink	Europa island as sink of Madagascar and source for mainland	MOZ6 ← → EUR ← MAD3	−349,046.26	1	1
	Stepping-stone	Bidirectional	MOZ6 ← → EUR ← → MAD3	−557,674.50	4	0
	Stepping-stone	Unidirectional from West to East	MOZ6 → EUR → MAD3	−368,883.09	2	0
	Stepping-stone	Unidirectional from East to West	MOZ6 ← EUR ← MAD3	−374,936.75	3	0

Note: The model with highest support is highlighted in grey. Connected populations with ←→ referring to bidirectional and → or ← to unidirectionality; C = model choice based on Bezier log-marginal likelihood values; and P = model probability based on C = 1.

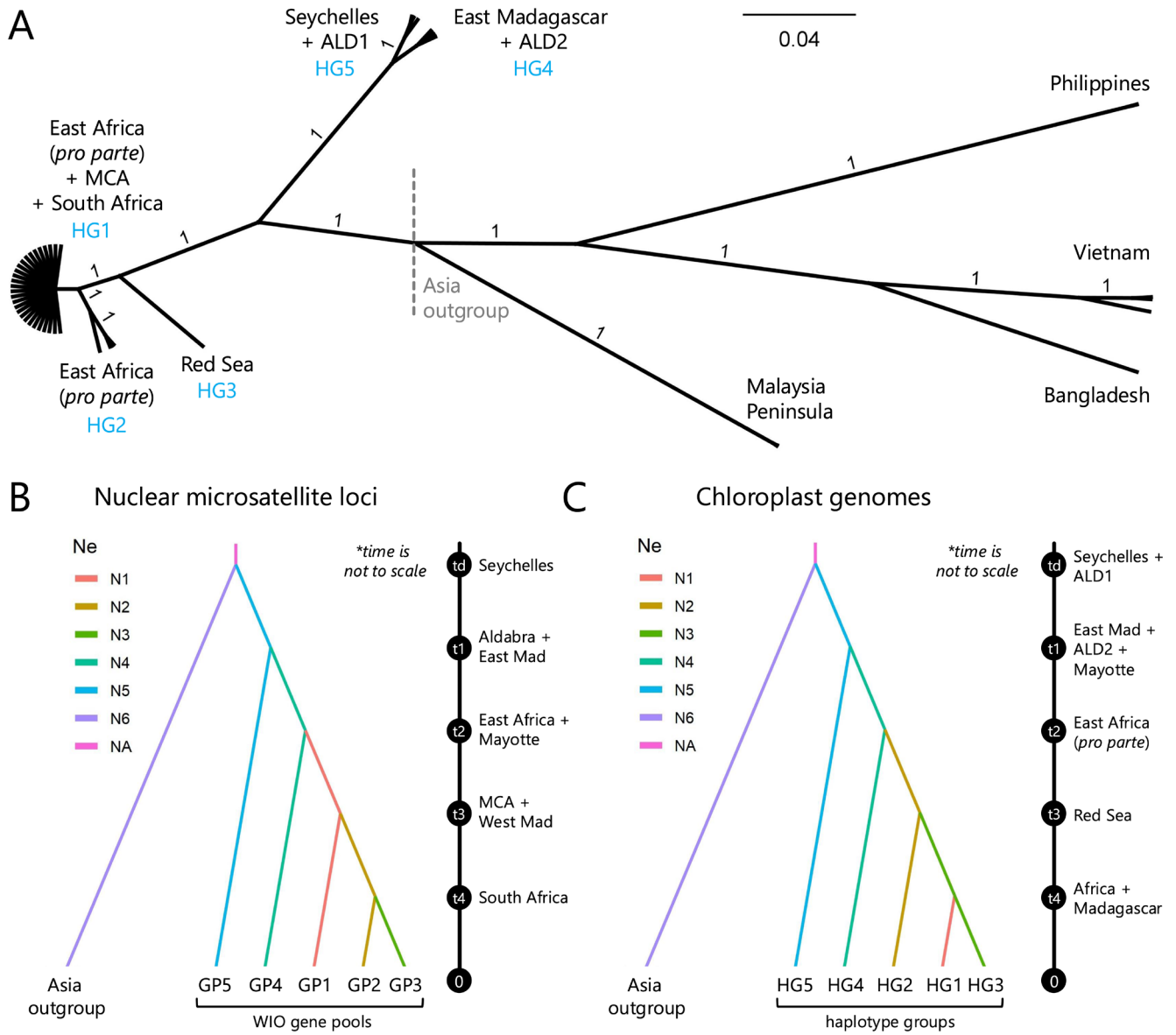

FIGURE 4 | Phylogenetic relationships of *Avicennia marina* in the WIO relative to Asian outgroup. (A) Maximum Likelihood Bayesian tree showing two haplogroups each of the western (HG1, HG2) and eastern (HG4, HG5) WIO, and a related HG3 of the Red Sea. (B) Most likely origin model from a DIYABC-RANDOM FOREST analysis with subsequent divergence times (t) of five microsatellite gene pools. (C) Most likely origin model from a DIYABC-RANDOM FOREST analysis with subsequent divergence times (t) of five haplotype groups.

values between 719 and 1352 (Figure S3.3). Posterior density estimates, using a generation time of 3 to 5 years, suggest divergence times of roughly (Table 4) $t_4 = 3$ to 5 kya for GP3 (South African range edge), $t_3 = 8$ to 12 kya for GP2 (MCA), and $t_2 = 14$ to 23 kya for GP1 (East Africa) as shown on the map (Figure 2A).

3.8 | Haplotype Diversity, Chloroplast Mutations and Evolutionary Units

After removing NUPTs, 87 mutations were retained in 41 WIO individuals—45 substitutions (transitions or transversions) and 42 mononucleotide repeats or indels. When including outgroups from the Red Sea and Southeast Asia, 342 mutations were identified: 223 substitutions and 119 mononucleotide repeats or indels (Appendix S5).

3.9 | Phylogenetic ML Tree

The ML tree (Figure 4A) revealed two main evolutionary units. The western WIO group includes populations from Kenya, Tanzania, Mozambique, South Africa, north and west Madagascar, and Europa Island (Figures 2B and 4A). The eastern WIO group comprises populations from the Aldabra Atoll, East Madagascar, and the Granitic Seychelles islands. Mayotte Island showed chloroplast capture from the eastern group.

3.10 | Haplonetwork

Five *A. marina* haplogroups from the WIO differed markedly from those in the Malaysian Peninsula and other Southeast Asian regions (Figure 2B). These haplogroups partly aligned

TABLE 4 | Approximate posterior distribution of parameters obtained from Bayesian origin models of nuclear microsatellite gene pools (see Figure 4B) and chloroplast haplogroups (see Figure 4C) obtained from DIYABC-RANDOM FORESTS.

	Number of t generations			$t=3$ years			$t=5$ years		
Nuclear microsatellite loci									
Supported scenario 6 (see Figure 4B)	Median	Q 0.05	Q 0.95	Median	Q 0.05	Q 0.95	Median	Q 0.05	Q 0.95
t_d	15,452	6527	37,452	46,356	19,581	112,356	77,260	32,635	187,260
t_1	8103	4597	9844	24,309	13,791	29,532	40,515	22,985	49,220
t_2	4664	1881	7834	13,992	5643	23,502	23,320	9405	39,170
t_3	2397	899	4780	7191	2697	14,340	11,985	4495	23,900
t_4	935	215	3572	2805	645	10,716	4675	1075	17,860
Chloroplast genome mutations (t_i and t_v)									
Supported scenario 4 (see Figure 4C)	Median	Q 0.05	Q 0.95	Median	Q 0.05	Q 0.95	Median	Q 0.05	Q 0.95
t_d	21,836	7972	41,820	65,508	23,916	125,460	109,180	39,860	209,100
t_1	15,146	5148	28,005	45,438	15,444	84,015	75,730	25,740	140,025
t_2	9991	2131	21,504	29,973	6393	64,512	49,955	10,655	107,520
t_3	12,088	1912	22,724	36,264	5736	68,172	60,440	9560	113,620
t_4	4059	967	8724	12,177	2901	26,172	20,295	4835	43,620

Note: Both models of nuclear microsatellites and of chloroplast sequences (t_i transitions and t_v transversions) contain similar parameters but their t_d and t_1 to t_4 may comprise different population groups. We consider a generation time of approximately 3 to 5 years for *Avicennia marina*.

with the nuclear microsatellite-based genetic structure. The five haplogroups (Figure 2C), each comprising related haplotypes, showed highest diversity (HG1 and HG2) in East Africa. HG2 was widespread and maternally linked most populations across the western WIO. HG3 was specific to the Red Sea, HG4 occurred in ALD1, East Madagascar, and Mayotte, and HG5 was found in the Seychelles and in ALD2. The two divergent haplogroups in Aldabra matched the presence of more than two alleles in nuclear microsatellites (see 3.1), suggesting multiple colonisation events. Similarly, the two haplogroups along East Africa reflect either local mutations or, more likely, multiple colonisation events (see further 3.11). HG2 in East Africa and HG3 in the Red Sea had similar numbers of mutational steps from their nearest shared node (Figures 2B and 2C), indicating a comparable divergence time.

3.11 | Origin Models of Five Haplogroups (Supported Scenario 4)

Among nine possible origin scenarios for the demographic evolution of *A. marina* haplogroups HG1 to HG5 in the WIO and Red Sea (Appendix S4, Figure S4.1), scenario 4 was best supported (27% votes, posterior probability = 0.54). This scenario proposes HG5 (Seychelles and ALD2) as the oldest maternal lineage, followed by successive divergences: HG4 (East Madagascar, ALD1, Mayotte), HG2 (partly East Africa), HG3 (Red Sea), and youngest HG1 (partly East Africa, MCA, South Africa) (Figures 4C and S4.2). The median divergence times ranged from $t_4 = 4059$ generations for the youngest lineage to $t_d = 21{,}836$ generations for the ancestral node (Table 4; Figures 4C and S4.3).

Assuming a generation time of 5 years (Table 4), haplogroups HG4 and HG5—found in the Seychelles, Aldabra, Mayotte, and East Madagascar—date to approximately 75,730 to 109,180 years BP, corresponding to the Late Pleistocene. Haplogroups HG3 (Red Sea) and HG2 (East Africa) are also referred to as Late Pleistocene (49,955 to 60,440 years BP), while HG1, present along the main African coast and MCA region, emerged more recently during the Holocene (20,295 years BP). The effective population sizes of the cpDNA lineages were estimated to range from $Ne = 3928$ to 5447 (Figure S4.3). Posterior density estimates were most robust for the oldest haplogroups. When using a generation time range of 3 to 5 years (Table 4), rounded median divergence estimates place HG1 at 12–20 kya, HG2 and HG3 at 30–60 kya and 30–50 kya, respectively, HG4 at 45–75 kya, and HG5 at 65–110 kya (Figure 2A). The inferred timing and origin of *A. marina* along the main African coastline and MCA (Figure 2A) are consistent across both nuclear microsatellite data ($t_2 = 14$–23 kya) and cpDNA sequences ($t_4 = 12$–20 kya). Notably, nuclear microsatellites proved more informative for tracing recent lineage divergence (LGM and Holocene), while

cpDNA mutations revealed insights into older, Late Pleistocene divergence events.

4 | Discussion

4.1 | Evolutionarily Significant Units

The WIO phylogeography of *Avicennia marina* features two distinct genetic groups: (1) the Seychelles, Aldabra, and East Madagascar; and (2) the main African coast and western Madagascar. Both groups represent distinct ESUs with different geographic origins and colonisation histories. While the broad geographical range of *A. marina* and its production of numerous propagules (Clarke 1992) suggest high dispersal potential, successful LDD across the Indian Ocean towards the WIO appears extremely rare, occurring perhaps once every 10,000–20,000 years. Such rare dispersal events likely exploit transient 'windows of opportunity', such as during glacial maxima, when lower sea-levels expose large areas of continental shelves and increase the number and size of islands (De Groeve et al. 2022). Such a scenario of enhanced resource populations and stepping stones was also proposed for *Rhizophora mucronata* (Triest, Sierens, and Van der Stocken 2021). Although Lagrangian-particle simulations based on high-resolution ocean circulation data suggest sporadic LDD between EIO and WIO for propagules with a 12-month floating period, a 6-month floating period would not suffice for direct jump dispersal to reach the African islands or mainland, and intermediate stepping stones would be necessary for successful transoceanic dispersal (Van der Stocken et al. 2019).

The cpDNA haplotype network spanning the WIO supports historical westward LDD events. Intermediate haplogroups found in the Seychelles, Aldabra and East Madagascar suggest ancient gene flow and highlight a Late-Pleistocene colonisation history. On the Seychelles, *A. marina* populations are highly genetically distinct and isolated—both from one another and from other WIO populations—with extremely low allelic diversity, evidence of genetic drift and signs of recent bottlenecks. Complete fixation of a single homozygous genotype in two populations points to limited founders followed by drift and biparental inbreeding, rather than selfing. Their isolation is reinforced by strong, directional ocean currents and geographic remoteness, which strongly limit propagule influx. Similar genetic isolation was reported for the mangrove crab *Neosarmatium meinerti* from Mahé, Rodrigues, Aldabra and Mauritius (Ragionieri et al. 2012).

A second colonisation event—dated roughly 20–35 kya—likely introduced a distinct maternal lineage to East Madagascar, with subsequent dispersal to Aldabra and Mayotte (the latter with chloroplast capture HG4 into nuclear GP1 and GP2). These events occurred against the backdrop of Pleistocene sea-level fluctuations, which shaped connectivity. Lower sea levels during the LGM exposed continental shelf areas, forming barriers to gene flow and altering surface-ocean circulation patterns. This created strong genetic discontinuities in mangroves from Southeast Asia towards the WIO (e.g., Gaither et al. 2011; Yang et al. 2017; Wee et al. 2020). Aldabra's then-expanded land area, in combination with additional source populations on emerged islands, likely increased Aldabra's capacity to intercept propagules from the EIO. In contrast, the present-day reduced size of the Seychelles Islands limits opportunities for successful colonisation. Thus, the presence of a rare and ancient ESU in restricted suitable sites on the Seychelles, Aldabra and East Madagascar underscores the conservation value of these populations. Rather than dismissing *A. marina* as a pantropical species of least concern, our data support the recognition of these isolated lineages as relics of Pleistocene colonisation via now-submerged dispersal corridors such as the Cargados Carajos Bank Ridge extending southward from the Seychelles (Hansen et al. 2017).

4.2 | Mixed Late Pleistocene and Holocene Origins

Since the LGM, sea-level fluctuations along the narrow continental shelf of the African coast caused less disruption to mangrove habitats over large geographic distances compared to other regions such as the Sunda Shelf, although a steep coast provides smaller accommodation space. *Avicennia marina* populations were able to shift with changing sea levels without encountering major geographic barriers along the main African coast. Nevertheless, bifurcation of the SEC near the Mozambique-Tanzania boundary, northward into the EACC along coasts of Tanzania and Kenya, and southward into the MCA, represents an important oceanographic barrier maintaining genetic differentiation. Dispersal from Madagascar via the Northeast Madagascar Current (NEMC) and historical northward currents—the Subtropical Convergence was up to 5° latitude further north during LGM (cf. Prell et al. 1980)—may have facilitated Late Pleistocene (~30–60 kya) colonisation of East Africa and the Red Sea. A distinct Red Sea haplogroup likely diverged from East African populations during that long period. Although less common, this older haplogroup is still present in locations like Lamu and Gazi (Kenya) and northern Tanzania. Subsequent Holocene dispersal (~12–20 kya by cpDNA; ~14–23 kya by microsatellites) introduced new lineages, mixing with remnants of the earlier gene pool. This admixture likely explains highest genetic diversity in East African *A. marina*. Microsatellite gene pools GP1 and GP2 overlap in Tanzania. Notably, haplogroup HG2, present in northern Tanzania, is absent from offshore islands (Zanzibar, Pemba, Mafia) and southern Tanzania suggesting two separate colonisation waves.

Avicennia marina populations of the Red Sea and the Persian/Arabian Gulf (PAG) showed lineage diversification with splitting time (40 to 295 kya) dating back to the Late and Middle Pleistocene during glacial periods of low marine connectivity, though followed by secondary contact among Red Sea and PAG populations (Friis et al. 2024).

This aligns well with our observation of mixed haplotypes of *A. marina* in East Africa. Southern Red Sea coral reefs appeared connected to regions in the Indian Ocean (Wang et al. 2019), whereas strong isolation of inner Red Sea populations from the WIO was reported for corals (van der Ven et al. 2021), fishes (DiBattista et al. 2016), arthropods (Iacchei et al. 2016), echinoderms (Vogler et al. 2008), molluscs (Hui et al. 2016), and sponges (Wörheide et al. 2008). We hypothesise that *Avicennia*

mangroves, along with other organisms, could establish in the northwestern peripheral region of the WIO much earlier than those along the continental African coast.

4.3 | Holocene Expansion

Our genetic data and demographic models suggest that *A. marina*'s genetic structure in the WIO is shaped more by historical gene flow than by strong demographic contractions. Most populations along the African coast, western Madagascar, Mayotte and Europa exhibit moderate genetic differentiation, consistent with ongoing connectivity. Four distant *A. marina* locations along Mozambique showed non-significant differentiation, suggesting a single gene pool (Amade et al. 2021). Gene flow patterns in Tanzania follow the northward EACC, while gene mixing between East Africa and western Madagascar occurs predominantly in an east-to-west direction. These findings are in line with trajectories of satellite-tracked drifters, showing that cross-channel transport is possible in both directions within a time span of 19 to 30 days, potentially driven by frontal zones between mesoscale eddies and interstitial waters (Hancke et al. 2014). This time span is within the range of propagule buoyancy periods reported for *A. marina* (Clarke and Myerscough 1991; Clarke et al. 2001).

Populations on Mayotte and Europa harbour high allelic diversity and share genetic affinities with both Malagasy and African sources, indicating multiple successful dispersal events. A recent Holocene expansion across the MCA was also reported for *R. mucronata* (Triest, Sierens, and Van der Stocken 2021; Triest, Van der Stocken, De Ryck, et al. 2021).

4.4 | Special Cases

Aldabra populations show higher allelic diversity than populations of the Granitic Seychelles, indicating more frequent colonisation events. Aldabra emerged ~125,000 years ago and its mangrove-suitable inner rim likely formed only ~4–5 kya (Braithwaite et al. 1973). Floating propagules could reach Aldabra from Madagascar or Africa in 5–7.5 days (Hnatiuk and Rudall 1985) facilitated by seasonal monsoon winds. However, cpDNA data suggest limited bidirectional gene flow. Two divergent haplotypes on Aldabra indicate successful colonisation events from sources related to East Madagascar (for ALD1) and the Seychelles (for ALD2). High allelic richness indicates multiple propagule arrivals from each. Strikingly similar to *A. marina*, Aldabra's *Rhizophora* populations show two spatially distinct lineages within the inner lagoon, and this occurs in the same site as *Avicennia*'s ALD2, harbouring a more ancient lineage related to the Seychelles (Triest, Sierens, and Van der Stocken 2021). Hence, this points to a multi-species colonisation event during a window of opportunity to disperse and colonise specific parts of the atoll.

Mayotte's *A. marina* populations exhibit nuclear microsatellite affinity with western Madagascar and Mozambique; however, cpDNA haplotypes link them to the East Madagascar or Aldabra's (ALD1) lineage. This suggests regular mixing of MCA gene pools, with Mayotte acting as a contemporary stepping-stone receiving propagules through the westward flowing SEC and Comoros Basin circulation (Hancke et al. 2014). Data from other islands of the Comoros archipelago can corroborate this MCA mixing hypothesis.

Range-edge populations showed reduced genetic diversity in Southeast Asia (Arnaud-Haond et al. 2006) and South Africa (De Ryck et al. 2016). Our data of South African populations suggest that a bottlenecked, youngest lineage (3–5 kya) dispersed across the Delagoa Bight Limpopo Current (DBLC). These share a main African haplogroup and are hypothesised to have established during a Holocene highstand (~4 kya), similar to patterns observed in Southeast Asia (Triest et al. 2025), when sea level rise may have facilitated mangrove dispersal upriver. Changes in surface-ocean circulation patterns during the LGM—like a weakened Agulhas current—may have further influenced dispersal opportunities (Prell et al. 1980). Estuary inlets in this region are often narrowed by strong wave action and highly mobile sediments, and during times of reduced river flow, they may remain closed to the ocean (Van Niekerk et al. 2020), thereby impeding the dispersal and establishment of mangrove propagules (Raw et al. 2023).

5 | Conclusions

This study presents the WIO phylogeography of *Avicennia marina*. We identified two distinct ESUs with different geographic origins and colonisation histories. Populations on the Seychelles, Aldabra, and East Madagascar experienced several Pleistocene colonisation events, while those along the African mainland and in the MCA were shaped by Holocene migrations that mirror present-day surface-ocean circulation patterns. Given the ecological importance of mangroves, appropriate conservation is needed for key evolutionary units and areas of high genetic diversity, particularly where gene pools mix. Remote island populations, often with very small and/or fragmented mangrove area and in many cases under development pressure, warrant special attention. LDD to these areas likely occurred only once or twice during the Holocene, or possibly as far back as the Late Pleistocene, when sea level was lower. Although present-day currents may facilitate LDD, such events are rare, and these remote populations remain highly vulnerable to isolation. This vulnerability is exacerbated by usual small and fragmented mangrove area, further threatened by sea level rise.

Author Contributions

L.T., D.D.R., N.K. and T.V.S. conceived the study; L.T., T.S. and D.D.R. collected the data; L.T. performed genetic data analysis and wrote materials, methods and results; L.T. and T.V.S. wrote introduction, discussion and made figures; all authors contributed to the discussion section.

Acknowledgements

We are grateful for help in collecting samples from Rosa Van der Ven, Liesbeth Vanheusden, Nele Schmitz, Cyrus Rumisha, Filip Huyghe, Hajaniaina Ratzimbazafy, Katy Beaver (Plant Conservation Action group PCA), Bruno Senterre (PCA), James Mougal (PCA), Nancy Bunbury (Seychelles Islands Foundation SIF), Janske van de Crommenacker (SIF), François Fromard and Marc Kochzius. This study was financed by Vrije Universiteit Brussel (BAS42 and OZR4102),

Marie-Curie International Research Staff Exchange Scheme 'Coastal Research Network on Environmental Changes' (EC grant agreement no. 247514) and scholarship 'Leopold III-fonds natuuronderzoek en natuurbehoud'.

Funding

This study was financed by Marie Skłodowska-Curie (MSCA) Staff Exchanges (European Research Executive Agency): 247514, Leopold III-fonds natuuronderzoek en natuurbehoud, Vrije Universiteit Brussel: BAS42; OZR4102.

Conflicts of Interest

The authors declare no conflicts of interest.

Data Availability Statement

Microsatellite data and chloroplast fragments that support the findings of this study can be found in the Dryad repository at https://doi.org/10.5061/dryad.hmgqnk9wr.

References

Alongi, D. M. 2002. "Present State and Future of the World's Mangrove Forests." *Environmental Conservation* 29: 331–349. https://doi.org/10.1017/S0376-89290-20002-31.

Amade, F. M. C., C. J. Carel J. Oosthuizen, and P. W. Chirwa. 2021. "Genetic Diversity and Contemporary Population Genetic Structure of *Avicennia marina* From Mozambique." *Aquatic Botany* 171: 103374. https://doi.org/10.1016/j.aquabot.2021.103374.

Arnaud-Haond, S., S. Teixeira, S. L. Massa, et al. 2006. "Genetic Structure at Range Edge: Low Diversity and High Inbreeding in Southeast Asian Mangrove (*Avicennia marina*) Populations." *Molecular Ecology* 15: 3515–3525. https://doi.org/10.1111/j.1365-294X.2006.02997.x.

Avise, J. C. 2000. *Phylogeography: The History and Formation of Species*. Harvard University Press.

Bandelt, H., P. Forster, and A. Röhl. 1999. "Median-Joining Networks for Inferring Intraspecific Phylogenies." *Molecular Biology and Evolution* 16, no. 1: 37–48. https://doi.org/10.1093/oxfordjournals.molbev.a026036.

Banerjee, A. K., W. Guo, S. Qiao, et al. 2020. "Land Masses and Oceanic Currents Drive Population Structure of *Heritiera littoralis*, a Widespread Mangrove in the Indo-West Pacific." *Ecology and Evolution* 10, no. 14: 7349–7363. https://doi.org/10.1002/ece3.6460.

Beerli, P. 2006. "Comparison of Bayesian and Maximum-Likelihood Inference of Population Genetic Parameters." *Bioinformatics* 22: 341–345. https://doi.org/10.1093/bioinformatics/bti803.

Beerli, P., and M. Palczewski. 2010. "Unified Framework to Evaluate Panmixia and Migration Direction Among Multiple Sampling Locations." *Genetics* 185: 313–326. https://doi.org/10.1534/genetics.109.112532.

Binks, R. M., M. Byrne, K. McMahon, G. Pitt, K. Murray, and R. D. Evans. 2019. "Habitat Discontinuities From Strong Barriers to Gene Flow Among Mangrove Populations, Despite the Capacity for Long-Distance Dispersal." *Diversity and Distributions* 25: 298–309. https://doi.org/10.1111/ddi.12851.

Braithwaite, C. J. R., J. D. Taylor, and W. J. Kennedy. 1973. "The Evolution of an Atoll: The Depositional and Erosional History of Aldabra." *Philosophical Transactions of the Royal Society of London. B, Biological Sciences* 266: 307–340. https://doi.org/10.1098/rstb.1973.0051.

Clarke, P. J. 1992. "Predispersal Mortality and Fecundity in the Grey Mangrove (*Avicennia marina*) in Southeastern Australia." *Australian Journal of Ecology* 17: 161–168. https://doi.org/10.1111/j.1442-9993.1992.tb00794.x.

Clarke, P. J., R. A. Kerrigan, and C. J. Westphal. 2001. "Dispersal Potential and Early Growth in 14 Tropical Mangroves: Do Early Life History Traits Correlate With Patterns of Adult Distribution?" *Journal of Ecology* 89: 648–659.

Clarke, P. J., and P. J. Myerscough. 1991. "Buoyancy of *Avicennia marina* Propagules in South-Eastern Australia." *Australian Journal of Botany* 39: 77–83. https://doi.org/10.1016/0304-3770(93)90021-N.

Collin, F. D., G. Durif, L. Raynal, et al. 2021. "Extending Approximate Bayesian Computation With Supervised Machine Learning to Infer Demographic History From Genetic Polymorphisms Using DIYABC Random Forest." *Molecular Ecology Resources* 8: 2598–2613. https://doi.org/10.1111/1755-0998.13413.

De Groeve, J., B. Kusumoto, E. Koene, et al. 2022. "Global Raster Dataset on Historical Coastline Positions and Shelf Sea Extents Since the Last Glacial Maximum." *Global Ecology and Biogeography* 31: 2162–2171. https://doi.org/10.1111/geb.13573.

De Ryck, D. J. R., N. Koedam, T. Van der Stocken, R. M. van der Ven, J. Adams, and L. Triest. 2016. "Dispersal Limitation of the Mangrove *Avicennia marina* at Its South African Range Limit in Strong Contrast to Connectivity in Its Core East African Region." *Marine Ecology Progress Series* 545: 123–134. https://doi.org/10.3354/MEPS11581.

DiBattista, J. D., M. B. Roberts, J. Bouwmeester, et al. 2016. "A Review of Contemporary Patterns of Endemism for Shallow Water Reef Fauna in the Red Sea." *Journal of Biogeography* 43, no. 3: 423–439. https://doi.org/10.1111/jbi.12649.

Do, B. T. N., N. Koedam, and L. Triest. 2019. "*Avicennia marina* Maintains Genetic Structure Whereas *Rhizophora stylosa* Connects Mangroves in a Flooded, Former Inner Sea (Vietnam)." *Estuarine, Coastal and Shelf Science* 222: 195–204. https://doi.org/10.1016/j.ecss.2019.04.005.

Donato, D. C., J. B. Kauffman, D. Murdiyarso, S. Kurnianto, M. Stidham, and M. Kanninen. 2011. "Mangroves Among the Most Carbon-Rich Forests in the Tropics." *Nature Geoscience* 4: 293–297. https://doi.org/10.1038/ngeo1123.

Duke, N. C. 1991. "A Systematic Revision of the Mangrove Genus *Avicennia* (Avicenniaceae) in Australasia." *Australian Systematic Botany* 4: 299–324. https://doi.org/10.1071/SB9910299.

Duke, N. C., M. C. Ball, and J. C. Ellison. 1998. "Factors Influencing Biodiversity and Distributional Gradients in Mangroves." *Global Ecology and Biogeography Letters* 7, no. 1: 27–47. https://doi.org/10.2307/2997695.

Excoffier, L., and N. Ray. 2008. "Surfing During Population Expansions Promotes Genetic Revolutions and Structuration." *Trends in Ecology & Evolution* 23, no. 7: 347–351. https://doi.org/10.1016/j.tree.2008.04.004.

Frankham, R. 2005. "Genetics and Extinction." *Biological Conservation* 126, no. 2: 131–140. https://doi.org/10.1016/j.biocon.2005.05.002.

Fraser, D. J., and L. Bernatchez. 2001. "Adaptive Evolutionary Conservation: Towards a Unified Concept for Defining Conservation Units." *Molecular Ecology* 10, no. 12: 2741–2752.

Friis, G., E. G. Smith, C. E. Lovelock, et al. 2024. "Rapid Diversification of Grey Mangroves (*Avicennia marina*) Driven by Geographic Isolation and Extreme Environmental Conditions in the Arabian Peninsula." *Molecular Ecology* 33: e17260. https://doi.org/10.1111/mec.17260.

Gaither, M. R., B. W. Bowen, T. R. Bordenave, et al. 2011. "Phylogeography of the Reef Fish *Cephalopholis argus* (Epinephelidae) Indicates Pleistocene Isolation Across the Indo-Pacific Barrier With Contemporary Overlap in the Coral Triangle." *BMC Evolutionary Biology* 11: 189. https://doi.org/10.1186/1471-2148-11-189.

Gallaher, T., M. W. Callmander, S. Buerki, S. Setsuko, and S. C. Keeley. 2017. "Navigating the 'Broad Freeway': Ocean Currents and Inland Isolation Drive Diversification in the *Pandanus tectorius* Complex (Pandanaceae)." *Journal of Biogeography* 44, no. 7: 1598–1611. https://doi.org/10.1111/jbi.12933.

Goudet, J. 2001. "FSTAT Version 2.9.3: A Program to Estimate and Test Gene Diversities and Fixation Indices (Update From Version 1.2, Goudet 1995): A Computer Program to Calculate F-Statistic." *Journal of Heredity* 86: 485–486. https://doi.org/10.1093/oxfordjournals.jhered.a111627.

Hancke, L., M. J. Roberts, and J. F. Ternon. 2014. "Surface Drifter Trajectories Highlight Flow Pathways in the Mozambique Channel." *Deep Sea Research Part II: Topical Studies in Oceanography* 100: 27–37. https://doi.org/10.1016/j.dsr2.2013.10.014.

Hansen, D. M., J. J. Austin, R. H. Baxter, et al. 2017. "Origins of Endemic Island Tortoises in the Western Indian Ocean: A Critique of the Human-Translocation Hypothesis." *Journal of Biogeography* 44: 1430–1435. https://doi.org/10.1111/jbi.12893.

Hardy, O. J., and X. Vekemans. 2002. "SPAGeDi: A Versatile Computer Program to Analyse Spatial Genetic Structure at the Individual or Population Levels." *Molecular Ecology Notes* 2: 618–620. https://doi.org/10.1046/j.1471-8286.2002.00305.x.

Hasan, S., L. Triest, S. Afrose, and D. De Ryck. 2018. "Migrant Pool Model of Dispersal Explains Strong Connectivity of *Avicennia officinalis* Within Sundarban Mangrove Areas: Effect of Fragmentation and Replantation." *Estuarine, Coastal and Shelf Science* 214: 38–47. https://doi.org/10.1016/j.ecss.2018.09.007.

He, Z., X. Feng, Q. Chen, et al. 2022. "Evolution of Coastal Forests Based on a Full Set of Mangrove Genomes." *Nature Ecology & Evolution* 6, no. 6: 738–749. https://doi.org/10.1038/s41559-022-01744-9.

He, Z., X. Li, M. Yang, et al. 2019. "Speciation With Gene Flow via Cycles of Isolation and Migration: Insights From Multiple Mangrove Taxa." *National Science Review* 6: 275–288. https://doi.org/10.1093/nsr/nwy078.

Hewitt, G. M. 2000. "The Genetic Legacy of the Quaternary Ice Ages." *Nature* 405, no. 6789: 907–913. https://doi.org/10.1038/35016000.

Hnatiuk, S. H., and P. Rudall. 1985. "Driftwood Genera Found on Aldabra Atoll." *Kew Bulletin* 40: 471–477. https://doi.org/10.2307/4109608.

Hu, Z., S. Temmerman, Q. Zhu, et al. 2025. "Predicting Nature-Based Coastal Protection by Mangroves Under Extreme Waves." *Proceedings of the National Academy of Sciences of the United States of America* 122, no. 12: e2410883122. https://doi.org/10.1073/pnas.2410883122.

Huelsenbeck, J. P., and F. Ronquist. 2001. "MRBAYES: Bayesian Inference of Phylogenetic Trees." *Bioinformatics* 17, no. 8: 754. https://doi.org/10.1093/bioinformatics/17.8.754.

Hui, M., W. E. Kraemer, C. Seidel, A. Nuryanto, A. Joshi, and M. Kochzius. 2016. "Comparative Genetic Population Structure of Three Endangered Giant Clams (Cardiidae: *Tridacna* Species) Throughout the Indo-West Pacific: Implications for Divergence, Connectivity and Conservation." *Journal of Molluscan Studies* 82: 403–414. https://doi.org/10.1093/mollus/eyw001.

Hülsen, S., L. E. Dee, C. M. Kropf, S. Meiler, and D. N. Bresch. 2025. "Mangroves and Their Services Are at Risk From Tropical Cyclones and Sea Level Rise Under Climate Change." *Communications Earth & Environment* 6: 262. https://doi.org/10.1038/s43247-025-02242-z.

Iacchei, M., M. R. Gaither, B. W. Bowen, and R. J. Toonen. 2016. "Testing Dispersal Limits in the Sea: Range-Wide Phylogeography of the Pronghorn Spiny Lobster *Panulirus penicillatus*." *Journal of Biogeography* 43, no. 5: 1032–1044. https://doi.org/10.1111/jbi.12689.

IUCN. 2024. "More Than Half of All Mangrove Ecosystems at Risk of Collapse by 2050, First Global Assessment Finds. Press Release 22 May, 2024 and Backed by 17 Regional IUCN Reports." https://ecoevorxiv.org/.

IUCN. 2025. "The IUCN Red List of Threatened Species. Version 2025.2." https://www.iucnredlist.org.

Leal, M., and M. D. Spalding, eds. 2024. *The State of the World's Mangroves 2024*. Global Mangrove Alliance. https://doi.org/10.5479/10088/119867.

Lee, S. Y., J. H. Primavera, F. Dahdouh-Guebas, et al. 2014. "Ecological Role and Services of Tropical Mangrove Ecosystems: A Reassessment." *Global Ecology and Biogeography* 23: 736–743. https://doi.org/10.1111/geb.12155.

Leigh, J. W., and D. Bryant. 2015. "PopART: Full-Feature Software for Haplotype Network Construction." *Methods in Ecology and Evolution* 6, no. 9: 1110–1116. https://doi.org/10.1111/2041-210X.12410.

Li, X., N. C. Duke, Y. Yang, et al. 2016. "Re-Evaluation of Phylogenetic Relationships Among Species of the Mangrove Genus *Avicennia* From Indo-West Pacific Based on Multilocus Analyses." *PLoS One* 11, no. 10: e0164453. https://doi.org/10.1371/journal.pone.0164453.

Lo, E. Y., N. C. Duke, and M. Sun. 2014. "Phylogeographic Pattern of *Rhizophora* (Rhizophoraceae) Reveals the Importance of Both Vicariance and Long-Distance Oceanic Dispersal to Modern Mangrove Distribution." *BMC Evolutionary Biology* 14: 83. https://doi.org/10.1186/1471-2148-14-83.

Madhavan, C., S. P. Meera, and A. Kumar. 2025. "Anatomical Adaptations of Mangroves to the Intertidal Environment and Their Dynamic Responses to Various Stresses." *Biological Reviews of the Cambridge Philosophical Society* 100, no. 3: 1019–1046. https://doi.org/10.1111/brv.13172.

Maguire, T. L., P. Saenger, P. Baverstock, and R. Henry. 2000. "Microsatellite Analysis of Genetic Structure in the Mangrove Species *Avicennia marina* (Forsk.) Vierh. (Avicenniaceae)." *Molecular Ecology* 9: 1853–1862. https://doi.org/10.1046/j.1365-294x.2000.01089.x.

Manni, F., E. Guerard, and E. Heyer. 2004. "Geographic Patterns of (Genetic, Morphologic, Linguistic) Variation: How Barriers Can Be Detected by Using Monmonier's Algorithm." *Human Biology* 76: 173–190. https://doi.org/10.1353/hub.2004.0034.

Manurung, J., B. M. Rojas Andrés, C. D. Barratt, et al. 2023. "Deep Phylogeographic Splits and Limited Mixing by Sea Surface Currents Governgenetic Population Structure in the Mangrove Genus *Lumnitzera* (Combretaceae) Across the Indonesian Archipelago." *Journal of Systematics and Evolution* 61: 299–314. https://doi.org/10.1111/jse.12923.

Mori, G. M., M. I. Zucchi, I. Sampaio, and A. P. Souza. 2015. "Species Distribution and Introgressive Hybridization of Two *Avicennia* Species From the Western Hemisphere Unveiled by Phylogeographic Patterns." *BMC Evolutionary Biology* 15: 61. https://doi.org/10.1186/s12862-015-0343-z.

Moritz, C. 1994. "Defining "Evolutionarily Significant Units" for Conservation." *Trends in Ecology & Evolution* 9, no. 10: 373–375. https://doi.org/10.1016/0169-5347(94)90057-4.

Ngeve, M., T. Van der Stocken, D. Menemenlis, N. Koedam, and L. Triest. 2016. "Contrasting Effects of Historical Sea Level Rise and Contemporary Ocean Currents on Regional Gene Flow of *Rhizophora racemosa* in Eastern Atlantic Mangroves." *PLoS One* 11, no. 3: e0150950. https://doi.org/10.1371/journal.pone.0150950.

Ochoa-Zavala, M., J. P. Jaramillo-Correa, D. Piñero, A. Nettel-Hernanz, and J. Núñez-Farfán. 2019. "Contrasting Colonization Patterns of Black Mangrove (*Avicennia Germinans*(L.) L.) Gene Pools Along the Mexican Coasts." *Journal of Biogeography* 46, no. 5: 884–898. https://doi.org/10.1111/jbi.13536.

Peakall, R., and P. E. Smouse. 2012. "GenAlEx 6.5: Genetic Analysis in Excel. Population Genetic Software for Teaching and Research—An

Update." *Bioinformatics* 28: 2537–2539. https://doi.org/10.1093/bioinformatics/bts460.

Piry, S., G. Luikart, and J. M. Cornuet. 1999. "Computer Note. BOTTLENECK: A Computer Program for Detecting Recent Reductions in the Effective Size Using Allele Frequency Data." *Journal of Heredity* 90: 502. https://doi.org/10.1093/jhered/90.4.502.

Prell, W. L., W. H. Hutson, D. F. Williams, A. W. H. Bé, K. Geitzenauer, and B. Molfino. 1980. "Surface Circulation of the Indian Ocean During the Last Glacial Maximum, Approximately 18,000 Yr B.P." *Quaternary Research* 14, no. 3: 309–336. https://doi.org/10.1016/0033-5894(80)90014-9.

Pritchard, J. K., M. Stephens, and P. S. Donelly. 2000. "Inference of Population Structure Using Multilocus Genotype Data." *Genetics* 155: 945–959. https://doi.org/10.1111/j.1471-8286.2007.01758.x.

Ragionieri, L., S. Fratini, and C. D. Schubart. 2012. "Revision of the *Neosarmatium meinerti* Species Complex (Decapoda: Brachyura: Sesarmidae), With Descriptions of Three Pseudocryptic Indo-West Pacific Species." *Raffles Bulletin of Zoology* 60: 71–87. https://doi.org/10.5281/zenodo.5449199.

Raw, J. L., T. Van der Stocken, D. Carroll, et al. 2023. "Dispersal and Coastal Geomorphology Limit Potential for Mangrove Range Expansion Under Climate Change." *Journal of Ecology* 111: 139–155. https://doi.org/10.1111/1365-2745.14020.

Sandoval-Castro, E., R. S. Dodd, R. Riosmena-Rodrıguez, et al. 2014. "Post-Glacial Expansion and Population Genetic Divergence of Mangrove Species *Avicennia germinans* (L.) Stearn and *Rhizophora mangle* L. Along the Mexican Coast." *PLoS One* 9: e93358. https://doi.org/10.1371/journal.pone.0093358.

Sheidai, M., L. Malekmohammadi, F. Ghahremaninejad, A. Danehkar, and F. Koohdar. 2024. "A New Computational Method to Estimate Adaptation Time in Avicennia by Using Divergence Time." *Scientific Reports* 14: 24158. https://doi.org/10.1038/s41598-024-74064-6.

Spalding, M., M. Kainuma, and L. Collins. 2010. *World Atlas of Mangroves*. Earthscan and James & James. https://doi.org/10.4324/9781849776608.

Srivastava, J., and V. Prasad. 2019. "Evolution and Paleobiogeography of Mangroves." *Marine Ecology* 40: e12571. https://doi.org/10.1111/maec.12571.

Su, G., Y. Huang, F. Tan, X. Ni, T. Tang, and S. Shi. 2007. "Conservation Genetics of *Lumnitzera littorea* (Combretaceae), an Endangered Mangrove, From the Indo-West Pacific." *Marine Biology* 150, no. 3: 321–328. https://doi.org/10.1007/s00227-006-0357-6.

Taberlet, P., L. Fumagalli, A. G. Wust-Saucy, and J. F. Cosson. 1998. "Comparative Phylogeography and Postglacial Colonization Routes in Europe." *Molecular Ecology* 7, no. 4: 453–464. https://doi.org/10.1046/j.1365-294x.1998.00289.x.

Takayama, K., Y. Tateishi, and T. Kajita. 2021. "Global Phylogeography of a Pantropical Mangrove Genus *Rhizophora*." *Scientific Reports* 11: 7228. https://doi.org/10.1038/s41598-021-85844-9.

Tomizawa, Y., Y. Tsuda, M. N. Saleh, et al. 2017. "Genetic Structure and Population Demographic History of a Widespread Mangrove Plant *Xylocarpus granatum* J. Koenig Across the Indo-West Pacific Region." *Forests* 8, no. 12: 480. https://doi.org/10.3390/f8120480.

Triest, L. 2008. "Molecular Ecology and Biogeography of Mangrove Trees Towards Conceptual Insights on Gene Flow and Barriers: A Review." *Aquatic Botany* 89, no. 2: 138–154. https://doi.org/10.1016/j.aquabot.2007.12.013.

Triest, L., A. Del Socorro, V. J. Gado, A. M. Mazo, and T. Sierens. 2021. "*Avicennia* Genetic Diversity and Fine-Scaled Structure Influenced by Coastal Proximity of Mangrove Fragments." *Frontiers in Marine Science* 8: 643982. https://doi.org/10.3389/fmars.2021.643982.

Triest, L., P. T. T. Hang, L. Q. Doc, et al. 2025. "Migration History of *Avicennia marina* Populations: A Legacy of Mangrove Expansion on the Sunda Shelf." *Frontiers Marine Sc.: Sec. Marine Evolutionary Biology, Biogeography and Species Diversity* 12: 1565908. https://doi.org/10.3389/fmars.2025.1565908.

Triest, L., B. Satyanarayana, O. Delange, K. K. Sarker, T. Sierens, and F. Dahdouh-Guebas. 2021. "Barrier to Gene Flow of Grey Mangrove *Avicennia marina* Populations in Peninsular Malaysia as Revealed From Nuclear Microsatellites and Chloroplast Haplotypes. Frontiers Conserv. Sc., Section Conservation Genomics. Research Topic: Integrated Phylogeography and Population Genomics of Coastal Ecosystems."

Triest, L., T. Sierens, and T. Van der Stocken. 2021. "Complete Chloroplast Genome Variants Reveal Discrete Long-Distance Dispersal Routes of *Rhizophora* in the Western Indian Ocean. Frontiers Conserv. Sc., Section Conservation Genomics. Research Topic: Integrated Phylogeography and Population Genomics of Coastal Ecosystems."

Triest, L., and T. Van der Stocken. 2021. "Coastal Landform Constrains Dispersal in Mangroves." *Frontiers in Marine Science* 8: 617855. https://doi.org/10.3389/fmars.2021.617855.

Triest, L., T. Van der Stocken, A. A. Akinyi, T. Sierens, J. Kairo, and N. Koedam. 2020. "Channel Network Structure Determines Genetic Connectivity of Landward–Seaward *Avicennia marina* Populations in a Tropical Bay." *Ecology and Evolution* 10, no. 21: 12059–12075. https://doi.org/10.1002/ece3.6829.

Triest, L., T. Van der Stocken, D. De Ryck, et al. 2021. "Expansion of the Mangrove Species *Rhizophora mucronata* in the Western Indian Ocean Launched Contrasting Genetic Patterns." *Scientific Reports* 11: 4987. https://doi.org/10.1038/s41598-021-84304-8.

Triest, L., T. Van der Stocken, T. Sierens, E. K. Deus, M. M. Mangora, and N. Koedam. 2021. "Connectivity of *Avicennia marina* Populations Within a Proposed Marine Transboundary Conservation Area Between Kenya and Tanzania." *Biological Conservation* 256: 109040. https://doi.org/10.1016/j.biocon.2021.109040.

Urashi, C., K. M. Teshima, S. Minobe, O. Koizumi, and N. Inomata. 2013. "Inferences of Evolutionary History of a Widely Distributed Mangrove Species, *Bruguiera gymnorrhiza*, in the Indo-West Pacific Region." *Ecology and Evolution* 3: 2251–2261. https://doi.org/10.1002/ece3.624.

Van der Stocken, T., D. Carroll, D. Menemenlis, M. Simard, and N. Koedam. 2019. "Global-Scale Dispersal and Connectivity in Mangroves." *Proc. Natl. Acad. Sci. USA* 116: 915–922. https://doi.org/10.1073/pnas.1812470116.

Van der Stocken, T., D. J. R. De Ryck, T. Balke, T. J. Bouma, F. Dahdouh-Guebas, and N. Koedam. 2013. "The Role of Wind in Hydrochorous Mangrove Propagule Dispersal." *Biogeosciences* 10: 3635–3647. https://doi.org/10.5194/bg-10-3635-2013.

van der Ven, R. M., J. F. Flot, C. Buitrago-López, and M. Kochzius. 2021. "Population Genetics of the Brooding Coral *Seriatopora hystrix* Reveals Patterns of Strong Genetic Differentiation in the Western Indian Ocean." *Heredity* 126: 351–365. https://doi.org/10.1038/s41437-020-00379-5.

Van Niekerk, L., J. B. Adams, N. C. James, et al. 2020. "An Estuary Ecosystem Classification That Encompasses Biogeography and a High Diversity of Types in Support of Protection and Management." *African Journal of Aquatic Science* 45: 199–216. https://doi.org/10.2989/16085914.2019.1685934.

Vogler, C., J. Benzie, H. Lessios, P. H. Barber, and G. Wörheide. 2008. "A Threat to Coral Reefs Multiplied? Four Species of Crown-Of-Thorns Starfish." *Biology Letters* 4, no. 6: 696–699.

Wang, Y., D. E. Raitsos, G. Krokos, J. Gittings, P. Zhan, and I. Hoteit. 2019. "Physical Connectivity Simulations Reveal Dynamic Linkages Between Coral Reefs in the Southern Red Sea and the Indian Ocean." *Scientific Reports* 9: 16598. https://doi.org/10.1038/s41598-019-53126-0.

Wang, Z.-Z., Z.-X. Guo, C.-R. Zhong, et al. 2022. "Genomic Variation Patterns of Subspecies Defined by Phenotypic Criteria: Analyses of the Mangrove Species Complex, *Avicennia marina*." *Journal of Systematics and Evolution* 60: 835–847. https://doi.org/10.1111/jse.12709.

Wee, A. K. S., A. M. E. Noreen, J. Ono, et al. 2020. "Genetic Structure Across a Biogeographical Barrier Reflect Dispersal Potential of Four Southeast Asian Mangrove Plant Species." *Journal of Biogeography* 47: 1258–1271.

Wee, A. K. S., K. Takayama, T. Asakawa, et al. 2014. "Oceanic Currents, Not Land Masses, Maintain the Genetic Structure of the Mangrove *Rhizophora mucronata* Lam. (Rhizophoraceae) in Southeast Asia." *Journal of Biogeography* 41: 954–964. https://doi.org/10.1111/jbi.12263.

Wörheide, G., L. S. Epp, and L. Macis. 2008. "Deep Genetic Divergences Among Indo-Pacific Populations of the Coral Reef Sponge *Leucetta chagosensis* (Leucettidae): Founder Effects, Vicariance, or Both?" *BMC Evolutionary Biology* 8: 24. https://doi.org/10.1186/1471-2148-8-24.

Ximenes, A. C., L. Ponsoni, E. E. Maeda, N. Koedam, and F. Dahdouh-Guebas. 2025. "Global Relationship Between Upwelling Intensities and Mangrove Distribution and Area." *Science of the Total Environment* 978: 179356. https://doi.org/10.1016/j.scitotenv.2025.179356.

Yan, Y. B., N. C. Duke, and M. Sun. 2016. "Comparative Analysis of the Pattern of Population Genetic Diversity in Three Indo-West Pacific *Rhizophora* Mangrove Species." *Frontiers in Plant Science* 7: 1434. https://doi.org/10.3389/fpls.2016.01434.

Yang, Y., J. Li, S. Yang, et al. 2017. "Effects of Pleistocene Sea-Level Fluctuations on Mangrove Population Dynamics: A Lesson From *Sonneratia alba*." *BMC Evolutionary Biology* 17: 22. https://doi.org/10.1186/s12862-016-0849-z.

Zu Ermgassen, P. S. E., T. A. Worthington, J. R. Gair, et al. 2025. "Mangroves Support an Estimated Annual Abundance of Over 700 Billion Juvenile Fish and Invertebrates." *Communications Earth & Environment* 6: 299. https://doi.org/10.1038/s43247-025-02229-w.

Supporting Information

Additional supporting information can be found online in the Supporting Information section. **Appendix S1:** ddi70147-sup-0001-supinfo.zip.